

MASS-SELECTED IR-VUV (118 NM) SPECTROSCOPIC STUDIES OF RADICALS, ALIPHATIC MOLECULES, AND THEIR CLUSTERS

Yongjun Hu,* Jiwen Guan,¹ and Elliot R. Bernstein^{2*}

¹MOE Key Laboratory of Laser Life Science & Institute of Laser Life Science, College of Biophotonics, South China Normal University, Guangzhou, 510631, China

²Department of Chemistry, Colorado State University, Fort Collins, Colorado, 80523-1872

Received 29 January 2013; revised 25 April 2013; accepted 25 April 2013

Published online in Wiley Online Library (wileyonlinelibrary.com). DOI 10.1002/mas.21387

Mass-selected IR plus UV/VUV spectroscopy and mass spectrometry have been coupled into a powerful technique to investigate chemical, physical, structural, and electronic properties of radicals, molecules, and clusters. Advantages of the use of vacuum ultraviolet (VUV) radiation to create ions for mass spectrometry are its application to nearly all compounds with ionization potentials below the energy of a single VUV photon, its circumventing the requirement of UV chromophore group, its inability to ionize background gases, and its greatly reduced fragmenting capabilities. In this review, mass-selected IR plus VUV (118 nm) spectroscopy is introduced first in a general manner. Selected application examples of this spectroscopy are presented, which include the detections and structural analysis of radicals, molecules, and molecular clusters in a supersonic jet. © 2013 Wiley Periodicals, Inc. Mass Spec Rev 32:484–501, 2013

Keywords: time-of-flight mass spectrometry; VUV ionization; gas-phase; clusters; IR spectroscopy; molecular beam

I. INTRODUCTION

Vibrational spectroscopy of molecules and clusters in supersonic jets is one of the most effective techniques for the investigation of their geometric structures and intermolecular interactions (Zwier, 1996; Ebata, Fujii, & Mikami, 1998; Buck and Huisken, 2000; Duncan, 2003; Lisy, 2006). Infrared (IR) plus ultraviolet (UV) double resonance spectroscopy, through fluorescence or multiphoton ionization (MPI) detection, has been developed into a useful technique for the study of intra- and inter-molecular geometrical structures of molecular assemblies in their neutral, unperturbed states (Brutschy, 2000a; Dessent and Müller-Dethlefs, 2000; Lisy, 2006). In this scheme, both resonance-enhanced multiphoton ionization (REMPI) and laser-induced fluorescence (LIF) can be employed to detect

molecules and unstable species (Lee et al., 1969; Ashfold et al., 1993).

Despite of the wide applications of the method, a double resonance IR–UV scheme requires the presence of an UV chromophore, which can be provided by an aromatic molecule (Lisy, 2006) or by an aromatic “tag” (Brutschy, 2000b). Thus the IR–UV technique is inapplicable for the unperturbed detection of species originally without an UV chromophore group. One way of circumventing this limitation is to employ the detection with single photon ionization in the VUV region instead, which may compromise the advantage of individual conformer selection. Under vacuum ultraviolet (VUV) radiation, species can be gently, near threshold ionized by a single photon as long as their vertical ionization energies are less than the VUV photon energy (Hanley & Zimmermann, 2009). The experimental results reveal this soft ionization process suppresses extensive molecular or cluster fragmentation (Dong et al., 2006; Belau et al., 2007): possible fragmentation following “soft,” single photon ionization is typically of only minor importance.

Recent studies demonstrate (Ng, 2002; Matsuda et al., 2010; Han et al., 2011a) that a VUV photon source coupled with IR absorption spectroscopy and time-of-flight mass spectrometry (TOFMS) is capable of rendering chemically relevant information on neutral and ionic molecules, clusters, and radicals. The vibrational frequencies and intensities of IR absorptions, such as modes involving OH, NH, and CH groups, are generally very sensitive probes of hydrogen bonding and other intra- and inter-molecular interactions, which make them excellent probes for investigation of detailed aspects of the structures of biologically relevant ions, radicals, and molecules.

Particularly in combination with modern electronic structure calculations, such as *ab initio* and density functional theory (DFT) calculations, IR-VUV-TOFMS has become a structural tool that is now being applied in a growing number of laboratories around the world: these include the groups of Ng (Ng, 2002; Woo et al., 2003; Bahng et al., 2006), Lee (Han et al., 2011a) and Fujii (Matsuda et al., 2006, 2009a, 2010). By the use of a tunable single-mode IR-OPO (optical parametric oscillator) laser and a comprehensive tunable VUV laser, together with the molecular beam and the pulsed field ionization (PFI) detection techniques, Ng et al. proposed an array of new photoion (PI)-photoelectron (PE) methods, that is, IR-VUV-PI and IR-VUV-PFI-PE methods. The studies shown there are good prospects for high-resolution spectroscopy studies of radicals and clusters and

Yongjun Hu and Jiwen Guan contributed equally to this work.

Contract grant sponsor: National Natural Science Foundation of China; Contract grant numbers: 20973067, 11079020, 21273083.

*Correspondence to: Yongjun Hu, College of Biophotonics, South China Normal University, Guangzhou, 510631, China; Elliot R. Bernstein, Department of Chemistry, Colorado State University, Fort Collins, Colorado 80523-1872.

E-mail: yjhu@scnu.edu.cn; erb@lamar.colostate.edu

their cations with the approach above. These works have been reviewed in 2009 (Ng, 2009). Recently, Mikami, Fujii, and Matsuda et al. have developed a stimulated Raman/VUV ionization approach (Matsuda et al., 2007) to complement their early IR/VUV results. They have written a review on the recent development of vibrational (including IR and Raman) spectroscopic techniques based on the VUV photoionization detection for jet-cooled clusters. And three detection schemes are described as the VUV-ID-IRPDS, IR-VUV-PIS, and SR-VUV-PIS, respectively. In addition, the vacuum-ultraviolet photoionization detection scheme was used to perform IR predissociation spectroscopy of unstable cluster cations such as unprotonated cluster cations of protic molecules (Matsuda et al., 2009b).

In recent years, we systematically studied structural, electronic, and chemical properties of radicals, organic and biological molecules and their clusters in the gas phase by combining mass selected and detected IR-VUV (118 nm) spectroscopy and theoretical calculations. In this review, the principles of this new spectroscopic approach first are introduced. Thereafter, we review the studies undertaken in our laboratories of jet cooled radicals, small organic alcohols and acids, aliphatic amino acids, and their clusters employing mass-selected, IR-VUV-TOFMS (118 nm) spectroscopy.

II. METHODS AND INSTRUMENTATION

A. Ion Preparation and Mass Spectrometry Techniques

The experimental apparatus employed to record VUV/TOFMS and IR spectra of species in a supersonic jet has been previously described in detail (Hu et al., 2006a). Generally, the gas phase species are generated by thermal vaporization and is seeded into a Ne/He (total pressure 3 atm) gas flow. The gaseous mixture is expanded into a vacuum chamber from a pulsed supersonic nozzle (Parker General Valve Series 9). A molecular beam, containing both monomeric species and clusters, is thus generated. The beam is collimated by a 1.5 mm diameter aperture skimmer located around 3.0 cm downstream of the nozzle, and then crossed perpendicularly by the VUV (118 nm) laser in the ionization region of the TOFMS. The counter-propagating IR laser beam is focused upstream or downstream of the VUV focal point by a 40 cm focal length lens. Figure 1 shows the whole experimental scheme for the IR plus VUV TOFMS.

B. Generation of VUV (118 nm) Radiation

Generation of coherent VUV light with rare gas or metal vapor has been explored since the 1970s and has been applied to LIF, photoionization, and photoelectron spectroscopies (Softley et al., 1987; Hart, Bourne, & Rayner, 1989; Yamanouchi & Tsuchiya, 1995; Ng, 2000). Compared with metal vapors, the main experimental advantage to rare gases is that they are much easier to handle, and can be housed in a room temperature gas cell, or expanded in a supersonic jet (Rettner et al., 1984). Nowadays atomic Xe, Kr, Ar are more commonly used. Generation of coherent VUV light can be accomplished by four-wave mixing or non-resonance frequency tripling (Kung, 1983). The principles and experimental arrangements for VUV genera-

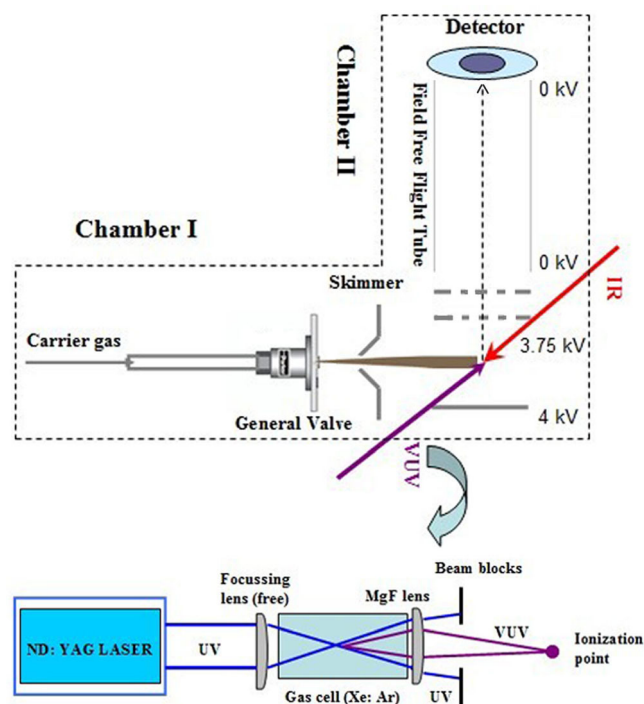


FIGURE 1. Experimental schematic diagram for the IR plus VUV spectroscopy.

tion have been discussed in several reviews (Hepburn, 1994; Lipson et al., 2000; Shi et al., 2002; Woodward et al., 2012). Briefly, it involves nonlinear optics using noble gases (typically xenon for the nonlinear, two photons near resonance and argon for phase matching) as the active medium using a laser to generate a high power source of coherent electromagnetic radiation. The induced polarization, \mathbf{P} , can be written as Taylor series in the laser electric field \mathbf{E} :

$$\mathbf{P} = \chi^{(1)}\mathbf{E} + \chi^{(2)}\chi\mathbf{E}\mathbf{E} + \chi^{(3)}\mathbf{E}\mathbf{E}\mathbf{E} + , \quad (1)$$

in which $\chi^{(n)}$ are the linear susceptibility and the n th order nonlinear susceptibility tensors of the medium, respectively. The noble gases have zero-valued $\chi^{(2)}$ coefficients. Therefore, the leading term is proportional to $\chi^{(3)}$. For the experiments reported here, coherent VUV (118 nm) is generated by third harmonic generation (THG, the output frequency is three times the input frequency). The input light is the third harmonic of an $\text{Nd}^{3+}/\text{YAG}$ laser fundamental output. For a focused Gaussian beam, the intensity of the 118 nm light ($\mathbf{I}_{3\nu}$)

$$\mathbf{I}_{3\nu} = N^2 |\chi^{(3)}(3\nu_{1\nu})|^2 I(\nu_{1\nu})^3 F(b\Delta k) \quad (2)$$

in which N is the number density of the Xe gas, $\chi^{(3)}(3\nu_{1\nu})$ is the third-order susceptibility, $I(\nu_{1\nu})$ is the intensity of the incident 355 nm light, and $F(b\Delta k)$ describes phase matching between the incident (355 nm) and third harmonic light (118 nm). This term depends on the confocal parameter b and the wave vector mismatch Δk . The confocal parameter $b = kw_0$ where w_0 is the minimum beam waist at the focus. For a Gaussian beam profile and tight-focusing geometry, the VUV output should be

independent of the confocal parameter b as long as $b \ll l$, where l is the length of the gas cell (Bjorklund, 1975). The wave vector mismatch

$$\Delta k = k_{3\omega} - 3k_{\omega} = \frac{2\pi n(\lambda_{3\omega})}{\lambda_{3\omega}} - 3 \frac{2\pi n(\lambda_{\omega})}{\lambda_{\omega}} \quad (3)$$

The indices of refraction, $n(\lambda_{3\omega})$ and $n(\lambda_{\omega})$, are those for the medium at the UV and VUV beam. In a gas, Δk is determined by $\Delta k = C \cdot N$ where C is the wavevector mismatch per atom between the generated radiation and the driving polarization. In the case of tight focusing of the laser beam into the center of the gas cell, the phase-matching factor

$$F(b\Delta k) = \begin{cases} \pi^2 (b\Delta k)^2 e^{(b\Delta k)^2/2}, & \Delta k < 0 \\ 0, & \Delta k \geq 0 \end{cases} \quad (4)$$

From the Equation (4), the nonresonant THG occurs in spectral regions for which the atomic medium (Xe) is negatively dispersive. One can differentiate the equation to get the maximum $b\Delta k = -4$: changing the beam focus to vary b (e.g., $b = 0.3, 0.12$ cm for focal length of the focusing lens $f = 150, 100$ mm, respectively), and/or changing N to alter Δk , to maximize the third-harmonic output $I_{3\omega}$. Since the refractive index is a strong function of λ near an atomic resonance line, coherent VUV generation can be maximized by adding different amounts of a positively dispersive buffer gas (Ar) to the Xe (typically Xe/Ar ratio of 1:10) (Hu, Fu, & Bernstein, 2006a). Lipson and co-workers experimentally showed that the maximum light output at an UV input energy of 14.6, 28.6, 41.4 mJ/pulse was achieved at a gas pressure of $\sim 105, 90, 80$ Torr, respectively (Shi et al., 2002).

In the home-made assembly device for the generation of 118 nm radiation, a dispersive MgF₂ lens is inserted into the optical path after the Xe/Ar cell to focus the 118 nm light and to disperse the 355 nm light. An additional MgF₂ prism can be employed to reduce the 335 nm intensity at the 118 nm focus further. The UV and VUV beam spatially separated due to the change in index of refraction of the lens. The MgF₂ lens is positioned so that the VUV beam is focused at the center of the ion source in the TOFMS while the UV beam is dispersed. The schematic diagram of the generation of VUV (118 nm) radiation is depicted in Figure 1.

C. Generation of Infrared Light

Over the past decade, a revolution has taken place in the performance of tunable IR bench-top laser systems. Laser systems based on nonlinear frequency down-conversion, such as optical parametric oscillation and amplification (OPO/OPA) and difference frequency generation (DFG) have matured considerably and are now commercially available. These developments have been made possible by the enhanced performance of novel birefringent materials and of solid state laser sources, used as pump source in nearly all OPO and DFG applications over the past decade (see e.g., Myers et al., 1995; Gerhards, Unterberg, & Gerlach, 2002; Gerhards, 2004; Diken et al., 2005).

A popular way of generating IR radiation in the 3 μ m wavelength range is through an optical parametric oscillator/amplifier (OPO/OPA) system (Laser Vision Co., Bellevue, WA, USA), pumped by a Nd³⁺/YAG laser. A type II KDP (KH₂PO₄)

doubling crystal is integrated into the OPO laser converting the Nd:YAG laser fundamental output to 532 nm. Two changeable sets of nonlinear crystals in the system are used to produce the outputs that provide wavelength coverage from 712 to 2,130 nm. With simple modifications to the optical layout, crystals of the second oscillator can be used to difference-frequency mix the output of the first oscillator with a portion of the 1,064 nm pump to provide additional wavelength coverage from 2.89 to 3.3 μ m. IR light output in the ranges covered is 3–5 mJ/pulse (2,500–4,000 and 3,500–7,500 cm⁻¹) with a bandwidth of 2–3 cm⁻¹ (broad band mode) or 0.4 cm⁻¹ (narrow band mode). The output between 7,800 and 10,990 cm⁻¹ has pulse energy of ~ 10 mJ/pulse and a bandwidth of ~ 2 cm⁻¹.

III. DETECTION SCHEMES

Three schemes for mass selective IR spectroscopy have been employed in the past: non-resonant ionization detected spectroscopy (NRID-IR), non-resonant ion dip (NRIDip-IR) spectroscopy, and VUV ionization detected IR predissociation (VUV-ID-IRPD) spectroscopy. The latter is based on single photon VUV photoionization detection. NRID- and NRIDip-IR spectroscopic schemes are applicable for neutral monomers and clusters, while the VUV-ID-IRPD is done only for ions.

A. Non-Resonant Ionization Detected Spectroscopy (NRID-IR)

The typical scheme for this technique is depicted in Figure 2a. In this scheme, introduction of IR radiation prior to the ionization step can have influences on two aspects of the detected mass spectra. A single VUV (10.5 eV) photon is not energetic enough to ionize jet cooled molecules or radicals, such as methanol (Fu, Hu, & Bernstein, 2006a), propanoic acid (Hu, Fu, & Bernstein, 2006c), peroxyacetyl radical (Hu, Fu, & Bernstein, 2006d), and methylthio radical (Han, Fu, & Lee, 2011b). When the IR laser is scanned to excite such jet cooled species to vibronic or vibrational excited levels, the total energy of $h\nu_{IR} + h\nu_{VUV}$ can be higher than the IE of selected species, and hence this neutral species can be ionized by absorption of a 10.5 eV and IR (*ca.* 3,000 cm⁻¹) photon. Therefore, the IR spectrum of this neutral species can be measured while monitoring the specific cation mass signal. Generally this detection scheme for monomers or

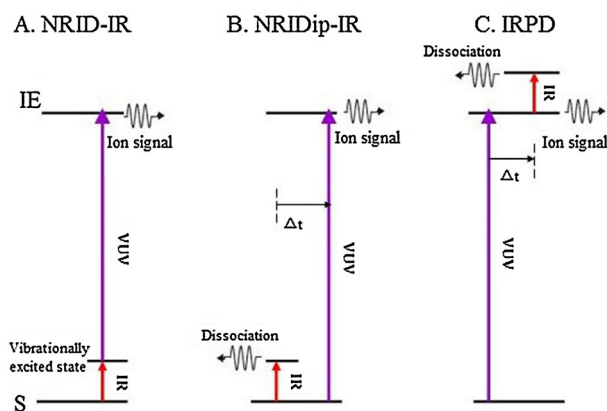


FIGURE 2. The schemes of mass selective (a) NRID-IR (b) NRIDip-IR (c) IRPD spectroscopic techniques.

radicals is termed non-resonant ionization detected spectroscopy (NRID-IR). NRID-IR spectroscopy is similar to NID-IR proposed by Fujii et al., previously (Ishiuchi et al., 1998).

Additionally, even though the energy of single VUV (10.5 eV) photon is enough to ionize a jet cooled species, the IR photon(s) added to the system can open or enhance fragmentation channels, which can be detected by VUV single photon ionization. As the IR laser is scanned to excite cooled molecules to high vibrational states of their ground electronic state prior to the VUV laser pulse and the fragment ion mass channel is monitored, the vibrational spectrum of the associated neutral molecule is obtained with high sensitivity due to the low background signal fluctuation in the fragment mass channel. In this case, the spectroscopic scheme is also called IR plus VUV non-resonant ionization and fragmentation detected (RIFD-IR) vibrational spectroscopy (Hu, Fu, & Bernstein, 2006a).

B. Non-Resonant Ion Dip IR Spectroscopy (NRIDip-IR)

For neutral clusters, absorbed IR photons can cause fragmentation of weakly bound clusters prior to the absorption of the VUV ionization photon (see Fig. 2b). Thus the intensity in mass channels of parent cluster ions as well as its daughter ions would be decreased due to IR predissociation of neutral clusters. In this scheme, IR spectra for a given cluster size can be well determined on the basis of the “sign” of the “ion-dip” detected in a specific mass channel while scanning IR wavelength. The measured IR spectra of the various species present in the sample can thus be employed to deduce qualitative information concerning cluster structure and intermolecular interactions (Fu, Hu, & Bernstein, 2006a; Hu, Fu, & Bernstein, 2006b).

C. VUV Ionization Detected IR Predissociation Spectroscopy (IRPD)

In this scheme (see Fig. 2c), the tunable IR light pulse is introduced with a delay time following the VUV laser pulse. A mass selected IR spectrum of a cluster cation or fragmented cluster cation is thus obtained as an ion dip spectrum. This detection method can in turn deduce the structure and dynamic information of cluster cations

with the aid of theoretical calculations. Recently, Matsuda and co-workers (e.g., Yamada et al., 2005; Matsuda et al., 2006) used the IRPD scheme with a time-of-flight mass spectrometer and/or tandem quadrupole mass spectrometer. With this latter approach, the parent cluster cations can be observed and monitored, as well as the fragment cation.

IV. COMPUTATIONAL METHODS

To interpret the experimental data from monomers or clusters, calculations of structure and molecular and intermolecular vibrations must be undertaken (Zwier, 1996). Geometry optimizations and harmonic frequency calculations are generated at both the MP2 (*ab initio*) and B3LYP (DFT) levels. Structural energies are corrected for zero point energy (ZPE) and/or basis set superposition error (BSSE), and harmonic frequencies are scaled by the ratios of experimental and theoretical OH stretches of model molecules to cover anharmonic effects. All calculational results discussed in this review are obtained using the Gaussian program package.

V. INVESTIGATION OF RADICALS, MOLECULES, AND THEIR CLUSTERS

A. Radicals

Owing to the reactive nature of radicals, it is difficult to prepare a pure sample of radicals in abundance. Generally, there are two methods to generate radicals from closed-shell precursors in the gas phase, that is, pyrolysis and photolysis (see Fig. 3). For some specific radicals, these two techniques are interchangeable. We have employed both of these techniques for the generation of methoxy, benzyl, methyl, cyclopentadienyl, NCO, and other radicals (Shang, Moreno, & Bernstein, 1994; Fu, Hu, & Bernstein, 2005; Hu, Fu, & Bernstein, 2006b,f).

1. Generation and Detection of the Peroxyacetyl (PA) Radical

Organic peroxy radicals are suggested to be involved in a number of atmospheric processes: the production of

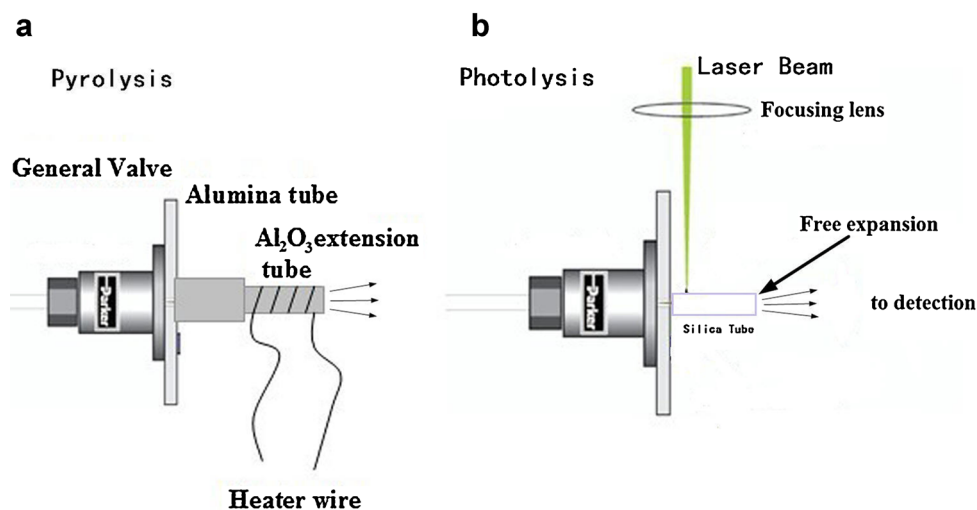


FIGURE 3. The scheme to generate radicals by the flash pyrolysis (a) and photolysis (b) techniques.

photochemical smog, the formation and precipitation of acids, and the emission of trace species, such as carbon monoxide and volatile organic compounds (Calvert et al., 1985; Claeys et al., 2004). As one of the most abundant and important organic peroxy radicals in the atmosphere, the peroxyacetyl radical (PA, $\text{CH}_3\text{C}(\text{O})\text{OO}\cdot$) can react with NO_2 to form peroxyacetyl nitrate (PAN, $\text{CH}_3\text{CO}(\text{OO})\text{NO}_2$): PAN can thus be considered a temporary reservoir and transport molecule for NO_x (Moxim, Levy, & Kasibhatla, 1996).

Figure 3a presents the scheme to generate the PA radical by the flash pyrolysis method which is coupled to a pulsed molecular beam (Hu, Fu, & Bernstein, 2006d). The basic flash pyrolysis/supersonic pulsed nozzle design was first reported by Kohn et al. (Kohn, Clauberg, & Chen, 1992). Briefly, a 4.5 mm o.d. and a 0.8 mm i.d. alumina tube with a length of 1 in. is attached to a General Valve Series 9 pulsed solenoid valve. Both the alumina tube and the nozzle are coaxial. Heater wire is wound around the Al_2O_3 extension tube and coated with alumina cement. A fast flow of the gas is achieved through this nozzle, which leads to short contact times with the heated wall, yielding correspondingly few secondary reactions.

Ab initio calculations show (Hu, Fu, & Bernstein, 2006f) that PA does not form a stable ion and only CH_3CO^+ is detected from photodissociation of PA recorded by photoionization mass spectra at 118 nm radiation. Figure 4a shows mass spectra of the thermal decomposition products of PAN in a flash pyrolysis tube generated by single-photon fragmentation and ionization with 118 nm light: under these conditions the ions CH_3CO^+ , CH_2CO^+ , and NO_2^+ are observed. With added IR radiation at 5578.2 cm^{-1} , which corresponding to the PA 0_0^0 transition, the peak intensity of the CH_3CO^+ mass channel signal increases by 30% while mass channel signals for CH_2CO^+ and NO_2^+ remained constant. These data implied that CH_3CO^+ comes from photodissociation of PA and the others do not. At 250°C , the intensities of peaks representing CH_3CO^+ are found to be maximum: this indicates that the maximum concentration of PA radicals in the molecular beam is generated at that temperature.

The scheme for the vibronic spectroscopic detection of PA in a supersonic jet is demonstrated in the Figure 4b. In the NIR spectra of PA, which is measured by monitoring the CH_3CO^+ mass channel signal, while scanning the near IR laser and presenting the 118 nm ionizing radiation simultaneously, a feature at *ca.* $5,582\text{ cm}^{-1}$ is observed. This peak is assigned to $0_0^0\text{ A} \leftarrow \text{X}$ electronic transition of PA. With the aid of *ab initio* calculations, the sequence of bands representing the vibrational modes O–O stretch 2^1 , COO bend 5^1 , and CCOO backbone 6^1 of the excited state vibronic transitions were identified. Rotational envelope simulation results show that the rotational temperature for PA on the ground state is *ca.* 55 K. An increase in rotational line width of the overtone of O–O stretch is observed and the O–O stretch anharmonicity estimated as 15.2 cm^{-1} .

2. Detection of the $\text{CH}_3\text{OO}\cdot$ Radical

As a common method for generation of radicals, photolysis relies on laser excitation of the precursor molecule to an electronic state that dissociates directly into the radical of interest plus a second fragment. A pulsed laser beam is focused by a cylindrical lens into the middle of a quartz tube (*ca.* 1 mm i. d. and 2 cm long) attached to the faceplate of the nozzle in line with the 0.5 mm orifice, as depicted in Figure 3b. The

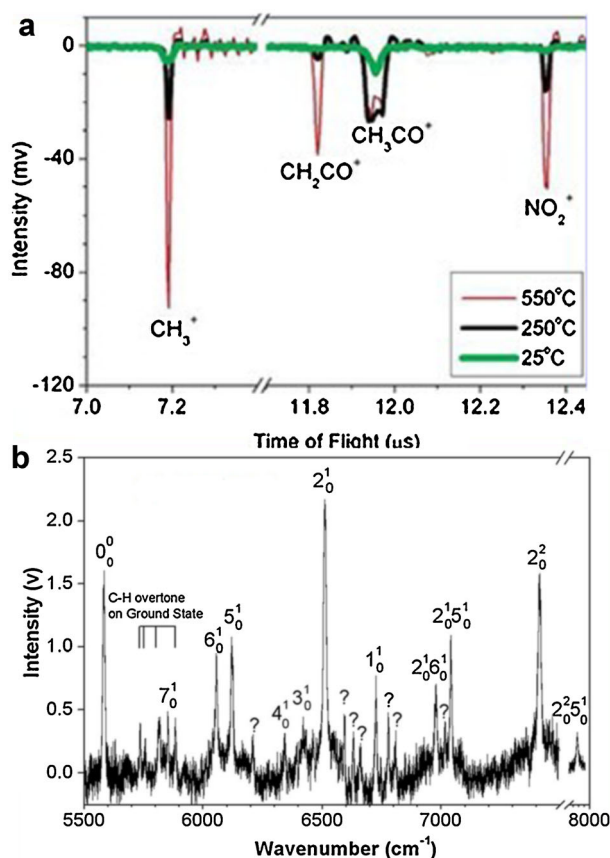


FIGURE 4. a: Mass spectra of the thermal decomposition products of PAN in a flash pyrolysis tube. b: Vibronic spectrum of PA radicals in a supersonic jet.

disadvantage of photolysis is the requirement for a laser as the light source to obtain a high enough photon flux for efficient radical generation: photolysis is thus more expensive than pyrolysis. Nevertheless, many radicals, such as methyl and methyl peroxy, have been successfully generated by photolysis and its vibrational spectra were thus studied (Fu, Hu, & Bernstein, 2005, 2006b).

In the report on the detection of the $\text{CH}_3\text{OO}\cdot$ radical, photolysis of acetone at 193 nm is used to generate the methyl radical. Thereafter, methyl peroxy radicals were produced by the initial production of a methyl radical with subsequent three body reaction with molecular oxygen prior to supersonic expansion into a vacuum system. Figure 5 presents the near IR spectrum of the methyl peroxy radical $\text{CH}_3\text{OO}\cdot$ for the $\text{A}^{\sim 2}\text{A}' \leftarrow \text{X}^{\sim 2}\text{A}''$ transition. The band centered at $7,381\text{ cm}^{-1}$ is attributed to the origin of the transition 0_0^0 . The features at 8,279 and $8,381\text{ cm}^{-1}$ are vibronic transition from the 0_0 level to excited ${}^2\text{A}''$ state vibrations.

Very recently, Lee and co-workers (Han, Fu, & Lee, 2011b) published spectra of the atmospherically important methylthio (CH_3S) radical. In that report, photolysis of CH_3SH produced CH_3S radicals that were ionized with (1 + 1) IR plus VUV (118 nm) photoionization and detected with TOFMS: the IR spectrum of CH_3S was obtained in the range $2,790\text{--}3,270\text{ cm}^{-1}$. This study further demonstrates the advantage and great potential of mass-selected IR-VUV (118 nm) spectroscopy for analysis of free radicals in a supersonic jet.

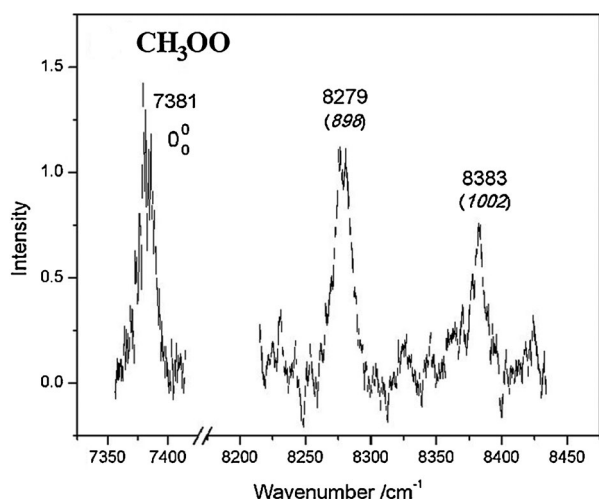


FIGURE 5. Electronic spectrum of the methyl peroxy radical for the $A^{\sim 2}A' \leftarrow X^{\sim 2}A''$ transition.

B. Organic and Biological Molecules

Instead of generating high concentrations of parent ion M^+ , conventional ionization techniques (electron impact, MPI, chemical ionization, fast ion bombardment) tend to yield high concentrations of fragment species for aliphatic organic and biological molecule precursors (Buzza, Snyder, & Castleman, 1996; Takayama, 1996; Grotheer et al., 2001; Jin, Daiya, & Kenttämaa, 2011). Nonetheless, VUV (118 nm) lasers are an excellent “soft,” generally non-fragmenting, ionization source for those molecules with minimal fragmentation (Lee et al., 1995; Shi et al., 1998; Tsai et al., 1999).

1. Methanol

The IP of methanol is *ca.* 10.8 eV, higher by ~ 0.3 eV than single photon energy at a 118 nm wavelength. Methanol's parent cations can only be observed in the mass spectra after the molecule neutral is vibrational excited under IR radiation. The IR spectrum of methanol in a jet cooled beam measured by IR plus VUV (118 nm) NRID-IR spectroscopy (Hu, Fu, & Bernstein, 2006b) is presented in Figure 6a. Features at approximately 3,684 and 7,196 cm^{-1} are assigned as the fundamental and first overtone of the OH stretch ν_1 , respectively (Rueda et al., 2005; Hunt et al., 1998). The four features at approximately 2,800–3,100 cm^{-1} are identified as the symmetric CH fundamental stretch ν_3 , low frequency vibrational combination bands, and the torsional tunneling asymmetric CH stretches (ν_2 and ν_9) (Hilbig & Wallenstein, 1983). The features at approximately 3,900 cm^{-1} are related to the combination bands of the CH stretches and the CO stretch fundamental ν_8 .

2. Ethanol

In like manner, the mid-IR spectrum of ethanol in a supersonic expansion is also obtained by monitoring the parent mass channel while the IR laser wavelength is scanned from 2,500 to 7,160 cm^{-1} . Note that the VUV non-resonant photon energy 10.49 eV is just 0.02 eV above the threshold of the ethanol ionization energy ($IE_{\text{ethanol}} = 10.47$ eV) (Hilbig & Wallenstein, 1983). This small excess energy is not sufficient for monomer

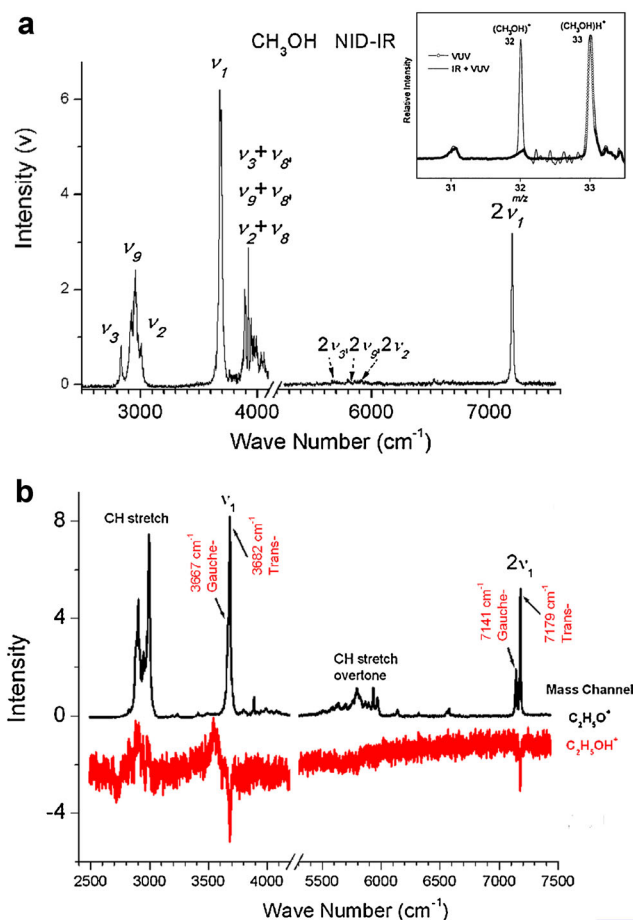


FIGURE 6. Mid-IR spectrum of the methanol (a) and ethanol (b) molecules in a jet cooled beam measured by IR plus VUV (118 nm) NRID-IR spectroscopy.

ions to dissociate and generate fragment ions. If additional energy is absorbed by the molecule around 0.3 eV or more, fragmentation channels can open (Kung & Lee, 1991). Thus the vibrational spectrum of neutral ethanol can be obtained by nonresonant ionization and fragmentation detected (RIFD-IR) vibrational spectroscopic scheme.

For lower background signal fluctuation, the results make clear the advantages of monitoring an IR induced dissociation product rather than the parent (see Fig. 6b). With this high sensitivity mass selective IR spectroscopy, features of OH stretches and overtone related to two ethanol conformers, that is, anti and gauche, can be clearly identified at 3,682, 7,179, and 3,667, 7,141 cm^{-1} in the observed IR spectra. Comparison with IR spectrum of neutral ethanol, the OH fundamental stretch for these ions (Hu, Fu, & Bernstein, 2006a) is found around a 210 cm^{-1} redshift, while no band shift in the fundamental CH stretch range is found for both neutral and ionic C_2H_5OH . The electron removed from the molecule in the above reaction is thus considered to come from the lone pair on the oxygen atom.

3. Organic Acids

Acetic acid and propanoic acid are two important organic acids. The VUV (10.5 eV) single photon is not energetic enough to

ionize either of them (Nist, <http://webbook.nist.gov/chemistry>). If the IR laser is scanned to excite the molecule to vibrational excited states of the ground electronic state, the total energy in the molecule of $h\nu_{\text{IR}} + h\nu_{\text{VUV}}$ is higher than the IE of these acids and the IR excited molecule then can be ionized or fragmented. With this detection scheme, IR spectra of organic acids in the gas phase can be detected. Measured IR spectra of acetic acid (Hu, Fu, & Bernstein, 2006e) and propanoic acid monomers (Hu, Fu, & Bernstein, 2006c) are shown in Figure 7. Assignment of each feature of the acetic acid IR spectra is labeled in the figure: features located at approximately 3,580 and 6,990 cm^{-1} are assigned to the OH fundamental stretch and its overtone, respectively. Four features located near 3,000 cm^{-1} have been identified as CH fundamental stretches, and the features at approximately 6,000 cm^{-1} are considered to be related to the CH stretch mode overtones. The medium intense features at approximately 4,000–5,400 cm^{-1} are assigned as combination bands.

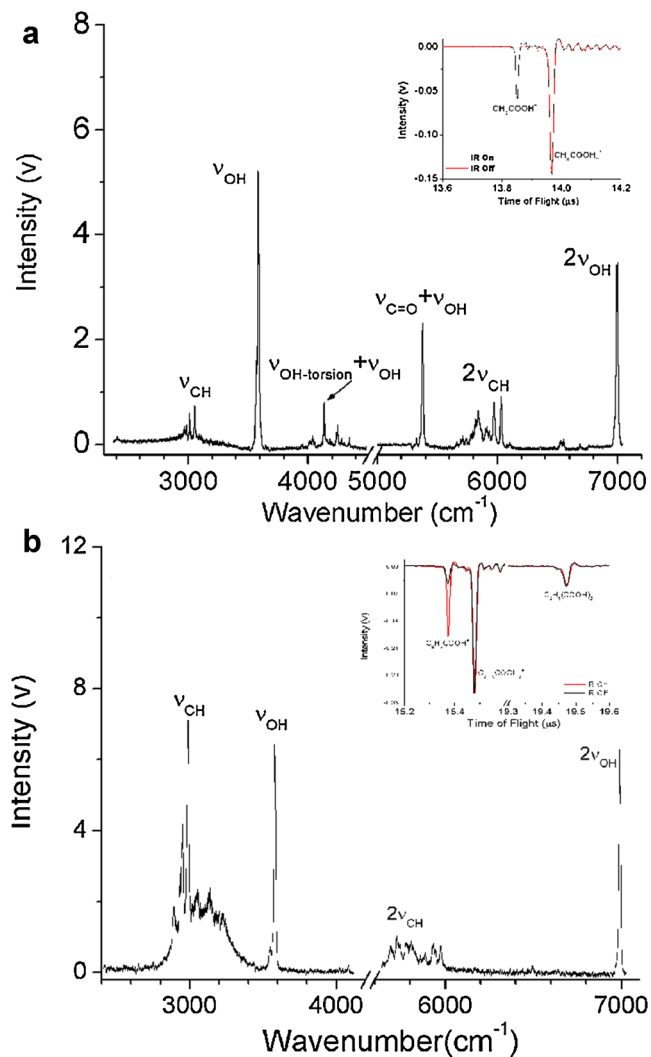


FIGURE 7. Mid-IR spectra of acetic acid (a) and propanoic acid (b) monomers in a supersonic jet.

4. Amino Acids

Structural and vibrational analyses of untagged aliphatic amino acids have also been undertaken by the IR/VUV approach (Hu & Bernstein, 2008). These biomolecules have very low vapor pressures at room temperature and can only be vaporized into the gas phase at sufficient concentrations by means of thermal evaporation or laser ablation. Investigations revealed that these biological samples would not be fragmented or decomposed by these evaporation techniques. For instance, the thermally fragile, low volatility valine molecules still remain intact in the gas phase at 220°C temperature (Svec & Clyde, 1965; Dong et al., 2006; Heinbuch et al., 2007; Guo, Bhattacharya, & Bernstein, 2009).

Among 20 important amino acids, only three of them (phenylalanine, tryptophan, tyrosine) have the aromatic ring group. Aliphatic amino acids, such as glycine, valine, leucine, and isoleucine must be substituted with a chromophore moiety (phenyl or indole) to be involved in two photon resonance ionization for detection. Gas phase studies of these amino acids in this way are reported by Ryan et al. (Ryan & Levy, 2001; Ryan, Gordon, & Levy, 2002), Mons et al. (Chin et al., 2005, 2006), Kleinermanns and co-workers (Hunig & Kleinermanns, 2004; Haber, Seefeld, & Kleinermanns, 2007), Abo-Riziq et al. (Abo-Riziq et al., 2006), Lee et al. (Lee et al., 2002), Simons and co-workers (Jockusch et al., 2004), and others (Chervenkov et al., 2004). Vibrational spectra of aromatic substituted amino acids are not identical to the vibrational spectra of the isolated gas phase aliphatic amino acids without the aromatic substituents (Cao & Fischer, 2000; Stepanian et al., 2001; Kaczor et al., 2006).

Single photon of 118 nm wavelength with the energy of 10.5 eV is known to be sufficient to directly ionize all amino acids. The ion in the present case is generated from the lone pair nitrogen orbital or possibly a mixed N–O orbital, which is the highest occupied molecular orbital (HOMO), and thus is directly involved with the amino acid $(\text{NH}_2)\text{-CHCOOH}$ molecular moiety. This leads to a structural rearrangement upon ionization possibly more complex than a simple proton transfer reaction and the energy that is released into the vibrational degrees of freedom of the ions (ΔH_{react}) by this reaction can cause the ions to fragment. This initial complication for IR/UV double resonance detection (no parent ion signal) also has an advantage, as the fragmentation patterns for the ionized amino acids turn out to be conformer dependent, as are the IR absorption spectra.

Combining IR and VUV radiations, the IR absorption spectra and fragmentation of the gas phase glycine, valine, leucine, and isoleucine have been studied (Hu & Bernstein, 2008; Bhattacharya et al., 2010). Results showed parent ions were not observed in these experiments while only fragment ions were detected in all the mass spectra due to fragmentation caused by deposition of the excess energy after VUV ionization. In present review, we take valine as the example to describe this approach for gas phase amino acids (Hu & Bernstein, 2008).

The obtained mass spectrum of valine is presented in Figure 8a. In this figure, two mass spectra are superimposed: the black line represents the mass spectrum of valine, irradiated by 118 nm photons and the red line represents the mass spectrum of valine obtained with both IR (with 3,000 cm^{-1}) and 118 nm radiations. The IR precedes the 118 nm pulse (10 nsec) by 30–50 nsec. As can be seen in the figure, the signals in mass

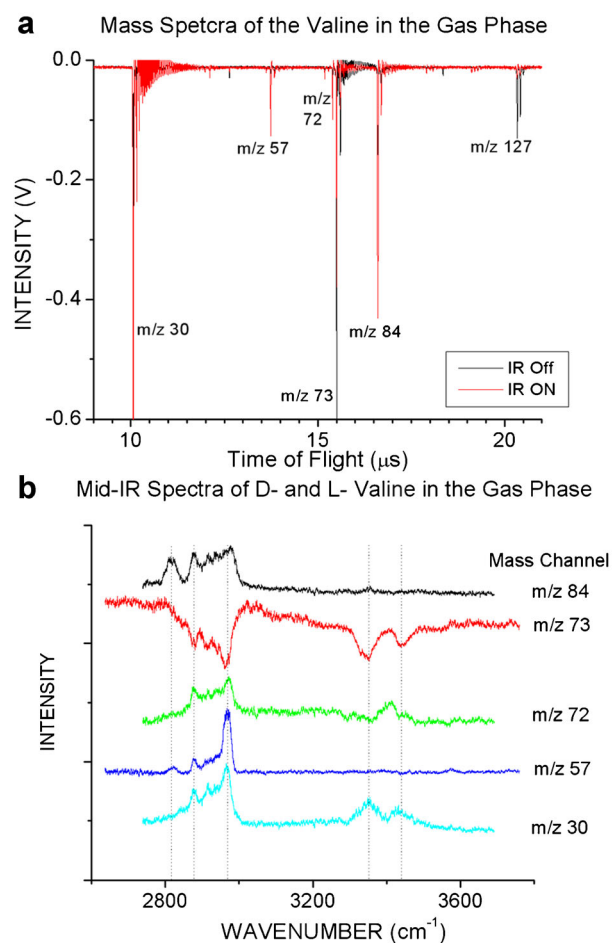


FIGURE 8. a: Time of flight mass spectrum of valine in the gas phase. b: Mid-IR spectrum of valine monomer measured by IR plus VUV spectroscopy.

channels 30, 57, 72, and 84 amu all increase in intensity with the addition of IR radiation ($3,000\text{ cm}^{-1}$), while the signal in mass channel 73 amu decreases in intensity with the addition of IR radiation. The mechanism for the observed fragmentation of valine upon ionization at 10.5 eV can be illustrated as followed: the ion is formed with enough excess energy to surmount any barrier to the overall structural rearrangement. This rearrangement provides enough energy to surmount the barriers to molecular fragmentation of the ion; the lowest barrier for the reaction would then be for the m/z species at 73 amu, with 72, 30, 84, and 57 amu species as the apparent ordered set of higher barrier mass channels for fragmentation. Absorption of IR radiation allows these higher barrier channels to become more populated and thus gain intensity at the expense of mass channel 73 amu intensity or population.

Figure 8b shows the IR spectrum obtained in the mass channels for valine fragments 84, 73, 72, 57, and 30 amu. Note three main points about these results. (I) Three distinct types of spectra are obtained. Mass channels m/z 84 and 57 amu display transitions only in the classical CH region ($2,900\text{ cm}^{-1}$), and the OH ($3,600\text{ cm}^{-1}$) and NH ($3,400\text{ cm}^{-1}$) mode absorptions are “missing.” (II) The IR spectra detected while monitoring mass channels 73 and 30 amu show two features in the “NH” range

($3,400\text{ cm}^{-1}$). The spectrum monitored in mass channel 73 amu is negative and therefore arises from a loss of intensity in this mass channel, while the IR spectrum obtained by monitoring mass channel 30 amu is positive and therefore arises from a gain in intensity in this mass channel. (III) The IR spectrum obtained by monitoring mass channel 72 amu evidences only one absorption feature in the NH region ($3,400\text{ cm}^{-1}$) in addition to the multiple absorption features in the classical CH mode region near ($2,900\text{ cm}^{-1}$).

Table 1 shows a suggestion for the ions observed in the different fragment mass channels, their associations with different isomers, and the observed vibrational modes and energies. The spectra detected by monitoring mass channels 57 and 84 amu belong to Isomer I (both NH_2 and OH moieties are involved in hydrogen bonding), the spectra detected in mass channels 73 and 30 amu belong to Isomer II (only the OH moiety is involved in hydrogen bonding), and the spectrum detected by monitoring mass channel 72 amu belongs to Isomer III (the OH moiety and one of the NH hydrogens are involved in hydrogen bonding).

The results for gas phase valine above, as an example for the studies on aliphatic amino acids, are shown to demonstrate that single photon ionization of aliphatic amino acids can be employed to detect IR spectroscopy of any (not just aromatic) isomeric amino acid in the gas phase. Thus, a UV chromophore is not required to be present to study the vibrational spectroscopy of biologically interesting molecules. The ionization step at 10.5 eV is without fragmentation, but the nascent parent ion undergoes a rearrangement releasing sufficient energy to surmount barriers to fragmentation. Each conformer of a given amino acid can have different fragmentation patterns associated with the intramolecular NH_2 and OH hydrogen bonding patterns for the isomers accessed. The above IR plus VUV study of aliphatic amino acid monomers provided vital information for understanding their intramolecular interactions, structures, and ion state behavior. The results on other aliphatic amino acid, such as glycine, leucine, also evidence this conclusion (Hunig & Kleinermanns, 2004; Haber, Seefeld, & Kleinermanns, 2007).

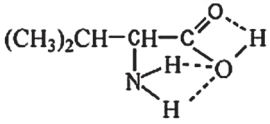
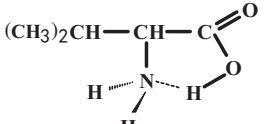
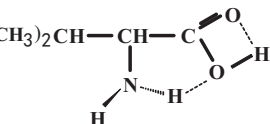
C. Clusters

Clusters offer a direct means to bridge the gap between gas and condensed phases and through them the essentials of gas and condensed phases can be understood at a molecular level (Zwier, 1996). Experimental observation and theoretical calculation can give general information about weakly bound systems and show that their characteristics undergo an evident conversion through system size evolution with regard stability, decomposition, ionization, and so on.

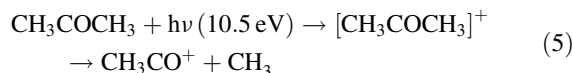
1. van der Waals Clusters (Taking Acetone Clusters as an Example)

Since acetone has two methyl groups and one carbonyl group, its clusters are expected to be an example of typical van der Waals molecular cluster systems, in which the general carbonyl-methyl interaction can be explored to enrich our understanding in terms of van der Waals interactions for chemical and biological systems. Recently, we have detected neutral acetone clusters $(\text{CH}_3\text{COCH}_3)_n$ ($n = 1-8$) using single photon VUV (118 nm) TOFMS (Guan et al., 2012a). The series of acetone

Table 1. Suggested fragmentation process under IR plus VUV radiation for the valine in the gas phase

Isomer Structures	Ionization and Fragmentation Process	Energies (cm ⁻¹) and Vibrational Modes
<p>I</p> 	<p>Cations <i>m/z</i> 84 $(CH_3)_2CHCH(NH_2)COOH \xrightarrow{h\nu} NH_2OH + (CH_3)_2CHCHCO^+$</p> <p>Cations <i>m/z</i> 57 $(CH_3)_2CHCH(NH_2)COOH \xrightarrow{h\nu} (CH_3)_2CH\bullet + OH\bullet + NH_2CHCO^+$ $\xrightarrow{h\nu} (CH_3)_2CH\bullet + NH_2\bullet + CHCOO^+$</p>	2800~3000, CH, OH, NH stretches
<p>II</p> 	<p>Cations <i>m/z</i> 73 $(CH_3)_2CHCH(NH_2)COOH \xrightarrow{h\nu} CO_2 + (CH_3)_2CHCHNH_3^+$</p> <p>Cations <i>m/z</i> 30 $(CH_3)_2CHCH(NH_2)COOH \xrightarrow{h\nu} (CH_3)_2CH\bullet + CO_2 + CH_4N^+ (CHNH_3^+)$</p>	2800~3000, CH, OH stretches 3346, Symmetric NH stretch 3436, Asymmetric NH stretch
<p>III</p> 	<p>Cations <i>m/z</i> 72 $(CH_3)_2CHCH(NH_2)COOH \xrightarrow{h\nu} COOH\bullet + (CH_3)_2CHCHNH_2^+$</p>	2800~3000, CH, OH stretches 3409, NH stretch

monomer and clusters cations $(CH_3COCH_3)_n^+$ with $n = 1$ to 8 and the fragment with $m/z = 43$ (i.e., CH_3CO^+) are observed (see Fig. 9). The fragment is considered to arise from the loss of a methyl group from bare acetone under single photon ionization, which is known to produce CH_3CO^+ ions and CH_3 radicals by the following steps:



For detection of IR spectra of neutral acetone clusters, IR light is introduced prior to VUV light and induces a resonant photodissociation of the clusters through vibrational excitation. Thus, the IR ion-dip spectra of the size-selected neutral cluster

are obtained by monitoring the signal intensity decrease of the corresponding cation, which is shown in Figure 10. The CO overtone is located at *ca.* 3,455 cm⁻¹ for the monomer, *ca.* 3,437 cm⁻¹ for the dimer, and *ca.* 3,434 cm⁻¹ for the trimer. The tetramer feature for this overtone is found at 3,433 cm⁻¹, shifted only 1 cm⁻¹ from that of the trimer.

In the C–H stretch region, the relative intensities of the three intense features, at *ca.* 2,936, 2,978, and 3,014 cm⁻¹, for the monomer and clusters are almost unchanged. The peak positions of the observed bands of the clusters are found to shift only slightly from those of free acetone. The lower energy band keeps the same position in the monomer and the clusters ($n = 2-4$), the second band has a slight blue shift, and the higher energy band red shift from monomer to clusters.

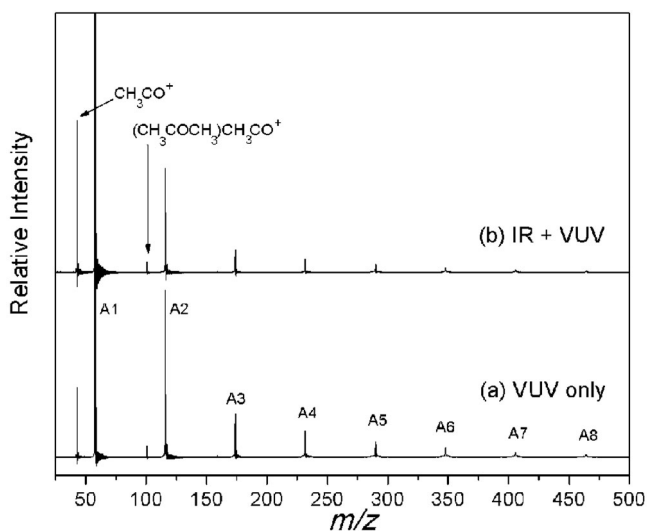


FIGURE 9. Mass spectra of the series acetone monomer and cluster cations $(CH_3COCH_3)_n^+$ ($n = 1-8$) with IR on and off.

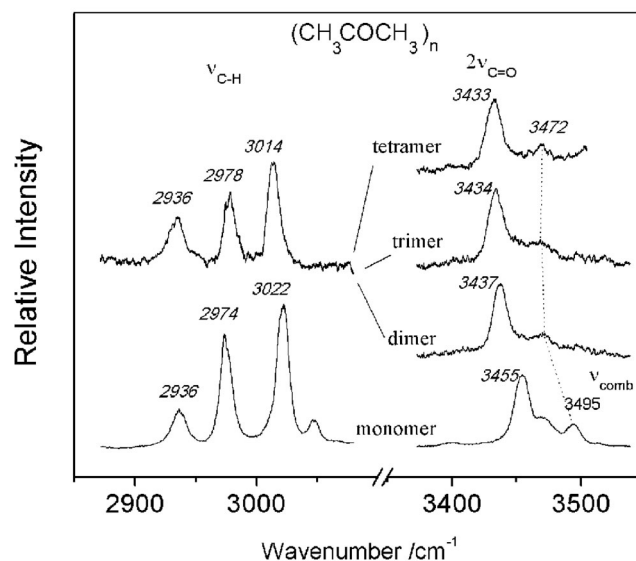


FIGURE 10. Mid-IR ion-dip spectra of the size-selected neutral acetone clusters.

Compared with the experimental IR spectra, the calculated results of DFT at the M06/6-31++G** level suggest that the dominant structures of the trimer and the tetramer are cyclic. The carbonyl groups would interact with the methyl groups in the formation of such acetone clusters. These weak interactions have been further confirmed by the use of hydrogen/deuterium substitution (Guan et al., 2012a).

Recently, Fujii and Matsuda et al. (Matsuda et al., 2006) have measured the IR spectrum of size selected acetone dimer employing a tunable coherent VUV light source. The results reveal that the acetone dimer has a C_{2h} symmetric structure, in which the acetone molecules stack with an antiparallel orientation of carbonyl groups. This group further explored the proton transfer process in the photoionization induced keto-enol tautomerization of hydrated acetone: IR spectra of the neutral and cationic acetone-water clusters are measured by IR plus VUV (118 nm) spectroscopy (Matsuda et al., 2010). Both the measured IR spectra and theoretical calculations identified that the catch and release catalytic action of a single water molecule is involved in the single photon ionization of the acetone-water complex under 118 nm radiation. Those findings, on the microscopic role of water catalysis contribute to the understanding of the role of water as intermediary in proton transfer/migration phenomena.

2. Solvated Aromatic Molecular Clusters (Taking Aniline-Methanol Complex as an Example)

Aniline is the simplest amine with an aromatic ring, and should be a generally good model for intermolecular interactions through an NH_2 or NH group (Jiang & Levy, 2002). The $S_1 \leftarrow S_0$ REMPI spectrum of the aniline-methanol complex consists of a broad structureless absorption; this fact limits the usefulness of the double resonance IR-UV scheme. Under VUV (118 nm) radiation, this complex can be ionized by a single photon in a single step, for which absorption to the excited intermediate S_1 state is not required.

Infrared (IR) spectra of neutral aniline-methanol clusters (Hu & Bernstein, 2009b), obtained by monitoring mass channels

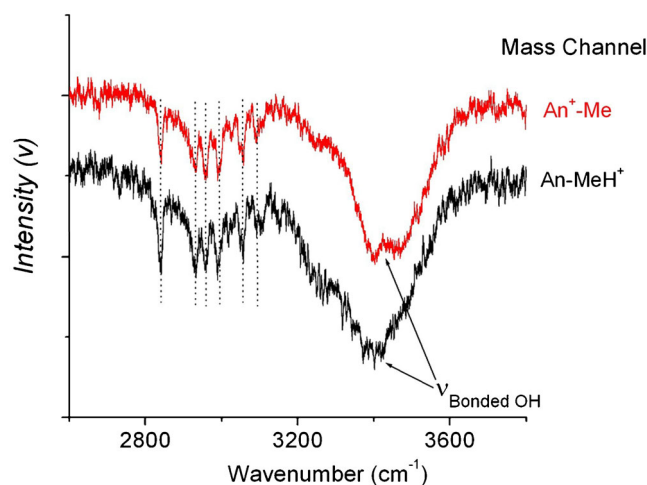


FIGURE 11. Mid-IR spectra of neutral cluster species of the aniline-methanol cluster.

m/z 125 and m/z 126, are presented in Figure 11. The vibrational mode energy predictions (see Table 2) for An-(Me) $_{1,2}$ agrees an assumption that the IR spectrum measured at the An-Meth $^+$ mass channel (125 amu) is associated with the neutral complex An-Meth, while that detected at the An-MethH $^+$ (126 amu) mass channel is associated with the neutral An-(Meth) $_2$ cluster. Table 2 revealed that broad dips at *ca.* 3,400 cm^{-1} are correlated with overlap of the hydrogen-bonded OH ($N \cdots H-O$) and free NH stretch modes. Features representing CH stretch modes *ca.* 2,900 cm^{-1} in the two IR spectra, which detected in the two mass channels (for An-(Meth) $_{1,2}$) respectively, correspond to each other very well. That suggests the CH groups are not involved in the interaction between molecules in the clusters. Features with frequencies higher than *ca.* 3,000 cm^{-1} are probably associated with the aromatic CH stretch vibrations of the aniline molecule (Hu & Bernstein, 2008), while those lower than *ca.* 3,000 cm^{-1} are related to the aliphatic CH stretch of methanol.

Table 2. Observed and calculated vibrational energies of the aniline $^+$ -CH $_3$ OH cluster cation and the aniline-(CH $_3$ OH) $_n$ neutral clusters for $n = 1, 2$ (in cm^{-1})

	Exp.	Cal. ^a	assignment
An-CH $_3$ OH $^+$	Unresolved, broadband, band center at 2950 cm^{-1}	2923	CH sym stretch (ν_3) of methanol
		2949	bond NH stretch of aniline
		3055, 3028	CH antisym stretch (ν_2 and ν_9) of methanol
		3066, 3074, 3079, 3087, 3092	CH sym and antisym stretch of the aromatic ring of aniline
		3438	3444
An-CH $_3$ OH	Unresolved, broadband, band center at 3444 cm^{-1}	3659	free OH stretch of methanol
		3380, 3471	NH sym and antisym stretch of aniline
		3465	bonded OH stretch of methanol
An-(CH $_3$ OH) $_2$	Unresolved, broadband, band center at 3413 cm^{-1}	3307, 3449	NH sym and antisym stretch of aniline
		3350, 3424	bonded OH stretch of methanol

^aTheory level B3LYP/aug-cc-pVDZ. A frequency factor of 0.96 is employed.

3. Hydrogen Bonded Clusters

Studies of hydrogen bonded clusters are of special interest because they can reveal the effects of structure and solvation behavior on the mechanisms of proton transfer reactions (Zwier, 1996; Ebata, Fujii, & Mikami, 1998; Yamanouchi & Tsuchiya, 1995). Clusters present a unique opportunity to study such details and model more complex systems that are fundamental to behavior in liquids, solids, and biological systems.

Due to their structural simplicity, methanol, and to a lesser extent, ethanol have received the most attention. Our successive studies (Fu, Hu, & Bernstein, 2006a; Hu, Fu, & Bernstein, 2006a,b) confirmed the conclusion that sequences of protonated cluster ions $(\text{CH}_3\text{OH})_{n-1}\text{H}^+$ observed in the TOFMS originate from their neutral parents $(\text{CH}_3\text{OH})_n$. Thus, mid-IR spectra obtained by employing IR plus VUV 118 nm nonresonant photodissociation spectroscopy and monitoring the ion signal in the $(\text{CH}_3\text{OH})_{n-1}\text{H}^+$ mass channel should reveal information of the neutral parent $(\text{CH}_3\text{OH})_n$ cluster. Figure 12a presents the mid-IR spectra of methanol clusters $(\text{CH}_3\text{OH})_n$ in the CH and OH stretch fundamental regions by monitoring the $(\text{CH}_3\text{OH})_{n-1}\text{H}^+$ mass channel for $n = 2, \dots, 8$. The top spectrum in this figure is of the methanol molecule obtained by employing IR plus VUV photons for enhancement of the ion signal. The neutral dimer spectrum, detected in the $(\text{CH}_3\text{OH})_2\text{H}^+$ mass channel, displays two main negative “dip” features located at approximately 3,676 and 3,572 cm^{-1} . These features imply that the structure of the dimer is not cyclic. The IR spectra of larger clusters $n \geq 3$ show only a broad hydrogen bonded OH stretch mode, and thus these larger clusters have a cyclic structure. Combining with theoretical predictions, a summary of the vibrational energies for $(\text{CH}_3\text{OH})_n$ $n = 1, \dots, 8$ are listed in Table 3. The theoretical results are consistent with closed, cyclic structures for clusters with $n \geq 3$. The other finding is that CH modes of these species are not significantly influenced by cluster formation. Thus the CH_3 group is not considered to be involved in the hydrogen bonding interaction network.

Recently, Lee and co-workers (Han et al., 2011a) have reported extensive observations of IR spectra of methanol clusters by the use of IR-VUV (118 nm) spectroscopy and consistent results with those mentioned above have been obtained. Additionally, new findings for the IR spectra of these clusters in the CH-stretching region are reported. In the region 2,800–3,050 cm^{-1} , they find bands near 2,845, 2,956, and 3,007 cm^{-1} for CH_3OH split into 2,823, 2,849, 2,934, 2,955, 2,984, and 3,006 cm^{-1} for $(\text{CH}_3\text{OH})_2$ that corresponding to proton donor and proton acceptor features, respectively, indicating that the methanol dimer has an open chain structure. In contrast, for $(\text{CH}_3\text{OH})_3$, the splitting diminishes and the bands near 2,837, 2,954, and 2,987 cm^{-1} became narrower, indicating a preferred cyclic structure.

Besides organic alcohol clusters, organic acid clusters are another simple hydrogen bonded species: examples here are acetic acid (Hu, Fu, & Bernstein, 2006e) and propanoic acid. Studies show that a well-defined cyclic structure with two hydrogen bonds is formed for gas phase acetic acid dimers. Mass selective non-resonant ion dip IR spectroscopy (Scheme B in Fig. 2) has been applied to determine the IR spectrum of the acetic acid neutral dimer in a supersonic expansion: the spectrum of the dimer A_2 is displayed in Figure 12b. The mass channels $(\text{CH}_3\text{COOH})\text{H}^+$ and $(\text{CH}_3\text{COOH})\text{COOH}^+$ are moni-

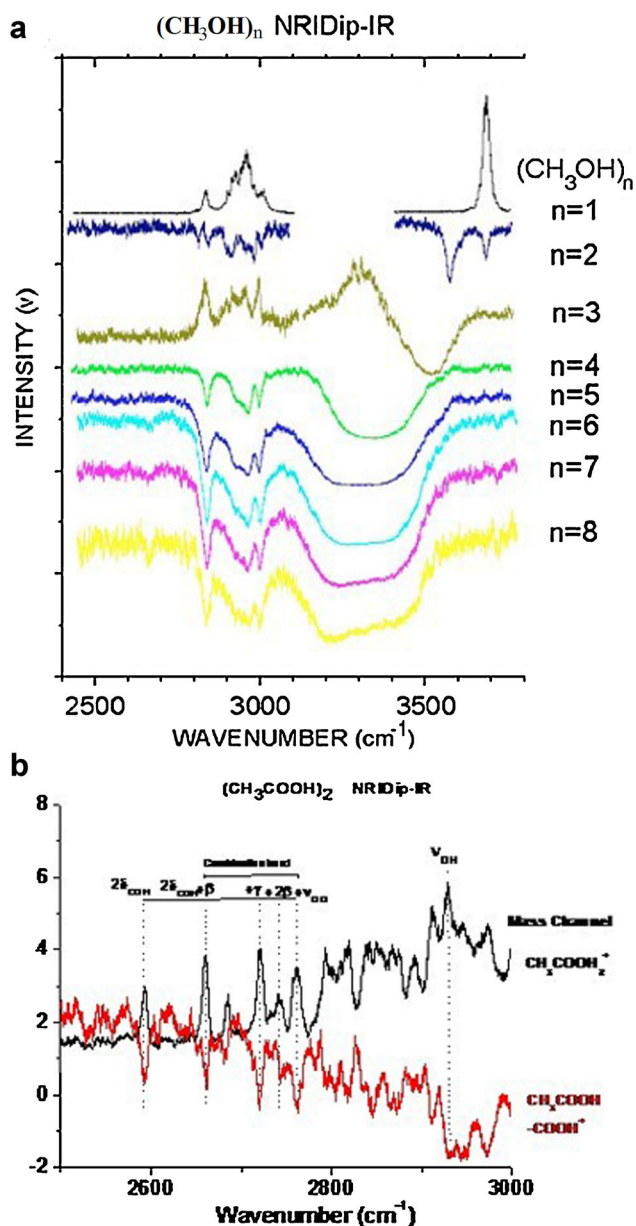


FIGURE 12. IR spectra of methanol (a) and acetic acid (b) hydrogen bond clusters in the CH and OH stretch fundamental regions.

tored and generate the same IR spectrum; this means that they arise from the same neutral precursor. These results are further confirmed by our recent report on study of acetic acid clusters by use of photoionization mass spectrometry measurements at the National Synchrotron Radiation Laboratory (NSRL) in Hefei, China (Guan et al., 2012b).

4. Amino Acid Clusters

With the IR/VUV (118 nm) ionization scheme, studies are extended to aliphatic amino acid clusters to investigate effects of intermolecular interactions on overall structures (Yamanouchi & Tsuchiya, 1995). Intra- and inter-molecular hydrogen bonds are well known to dictate the three-dimensional structures and reactivities of biological molecules. All biological processes

Table 3. Vibrational energies for neutral methanol cluster (cm^{-1})

$(\text{CH}_3\text{OH})_n$	CH stretch				OH stretch	
	ν_3	Combination or overtone	ν_9	ν_2	Resolved ^a	Band center (FWHM)
1	2837	2925	2956	3010	3684	3683.9
2					3576, ^d 3679 ^c	3612.9, 3758.6
3	2832	2914	2953	2995		3515 (142)
4	2839	2932	2962	2996		3339 (260)
5	2838	2928	2961	2995		3302 (307)
6	2839	2925	2960	2998		3317 (312)
7	2840	2925	2960	2997		3326 (340)
8	2837	2925	2966	2995		3322 (345)

^aFor $n = 1, 2$, features are resolved.^bFor $n = 3-8$, unresolved features of bonded OH stretches; FWHM: full width at half maximum.^cSee Hagemester, Gruenloh, and Zwier (1998).^dFree OH stretch in the dimer.^eBonded OH stretch in the dimer.

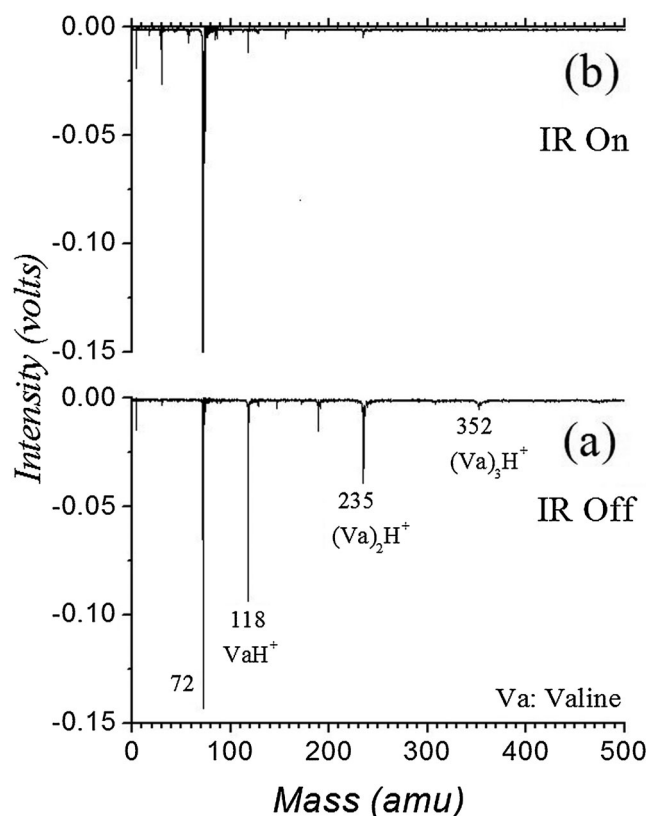
occur in the liquid phase, and our understanding of cluster behavior in the gas phase can help us to understand some condensed phase basic processes, as the description of cluster solvation effects help bridge the gap between gas and liquid phase structure and dynamics. Highly complicated hydrogen

bonding networks that govern peptide-peptide and protein-protein interactions can be analyzed at a very fundamental level through the investigation of amino acid clusters. Amino acid clusters are generated by increasing the gas phase sample concentration for supersonic expansion by direct thermal vaporized of the sample (Hu & Bernstein, 2009a).

Under 118 nm single photon ionization, prominent features in the TOF mass spectrum of valine clusters (see Fig. 13) appear at 72 amu (valine monomer fragment) (Ryan & Levy, 2001), 118, 235, 352, 469 amu ((valine) $_{n-1}\text{H}^+$, $n = 2-5$, fragments), and other mass channels (e.g., 147, 189, ... amu). The feature at 72 amu can be assigned to $(\text{CH}_3)_2\text{CHCH}(\text{NH}_2)^+$, that is, valine minus COOH. The mass channels $117 + 30$ and $117 + 72$ amu are expected for valine monomer fragmentation from a neutral dimer, trimer, tetramer, etc.

Figure 14 presents the mid-IR spectra (in the region 2,500–4,000 cm^{-1}) of high concentration neutral valine cluster system obtained by monitoring mass channels 118, 235, and the fragment valine mass channels, (valine) $(\text{NH}_2)\text{CHCH}(\text{CH}_3)_2^+$ (189 amu), (valine) NH_2CH_2^+ (147 amu), and $\text{NH}_2\text{CHCH}(\text{CH}_3)_2^+$ (72 amu). Obviously, the spectrum in mass channel 72 amu is correlated with valine monomers and fragmented valine monomers derived from valine clusters dissociated by absorption of an IR photon(s). The latter monomer species mass channel spectra arise from various clusters. Thereby, the IR spectrum detected in mass channel 72 amu should be related to both valine monomer and its clusters. As expected, this species has generated “positive” TOFMS and IR spectra, as shown in the figure: other cluster associated mass channels displayed “negative” IR spectra.

Since all cluster mass channels (>117 amu) displayed similar, negative IR absorption signals and the monomer fragment mass channel 72 amu displays a positive IR absorption signal, the observed spectra in the (valine) $_{n-1}\text{H}^+$ mass channels arise from the (valine) $_n$ neutral clusters. Absence of the free O–H stretching mode in the spectra of these clusters indicates that all the OH moieties are hydrogen bonded in the clusters,

**FIGURE 13.** TOF mass spectra of valine clusters under 118 nm single photon ionization with resonance (a) IR off (b) IR on.

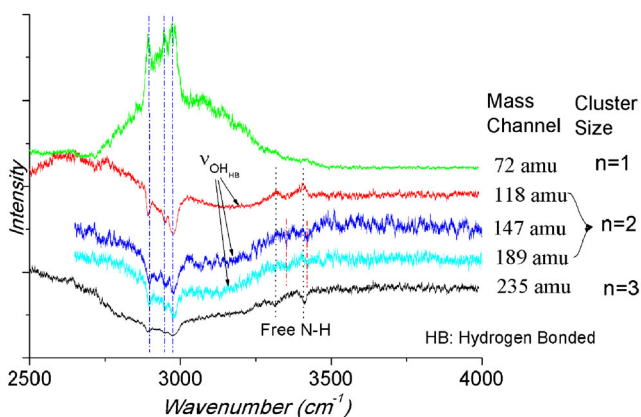


FIGURE 14. Mid-IR spectra of neutral valine clusters in the region 2,500–4,000 cm^{-1} .

while free NH stretching modes observed in the spectra suggest that the hydrogen atoms of the amino group are not directly involved in the hydrogen bonds holding the clusters together. In the presence of IR radiation, fragments 118, 147, and 189 amu probably all arise from both valine dimer and trimer, that is $(\text{valine})_{2,3}$. Nevertheless, other higher clusters are also potential parent species but concentrations, energetics, and absorption probabilities do favor the neutral dimer route. Note that the NH spectral regions in the 118 amu mass channel are different as detected in other mass channels in Figure 14. The features at 3,318 and 3,406 cm^{-1} that appear in the 118 amu mass channel can be related to “free” NH stretching modes of the neutral valine trimer (see Fig. 14, intensities decreasing in mass channel 235 amu). Nonetheless, these features do not appear in other potentially neutral trimer related mass channels amu 147 and 189: instead, two very weak features (marked in Fig. 14) are suggested as intensities decreasing at *ca.* 3,352 and 3,424 cm^{-1} . The origin of these latter peaks can be related to a dimer. The fact that they are slightly blue-shifted with respect to the “free” N–H peaks in the 118 amu mass channel indicates the absence of the O–H···N hydrogen-bonding configuration in the structure. Moreover, these peaks cannot be from the trimer or larger clusters. If they were, those features would be increased.

D. Ionic Clusters (Taking Acetic Acid Dimer Cation as an Example)

Making use of changes in a characteristic property of the ion, induced by the absorption of one or more photons, one can overcome the problem of low ion densities impeding the measurement of direct absorption spectra of ions. Such an approach is generally referred as an “action” spectroscopy method, which has greatly enhanced the applicability of, and the interest in, IR ion spectroscopy (Headrick, Bopp, & Johnson, 2004). Several excellent reviews on spectroscopy of ions have been documented in recent years: the application of IR spectroscopy of biomolecular ions and their solvation reviewed by Polfer and Oomens (2009), IR multiple photon dissociation (IR-MPD) in quadrupole ion traps by Brodbelt and Wilson (2009), high-resolution spectroscopy of cluster ions in tandem mass spectrometers by Bieske and Dopfer (2000). There are other reviews available on developments of IR spectroscopy of ions over the years (Duncan, 2003; Lisy, 2006; MacAleese & Maitre, 2007).

The recent development of vibrational spectroscopic techniques based on VUV photoionization enables observation of the IR spectra of simple and fundamental molecular clusters, both neutral and cations (Hu, Fu, & Bernstein, 2006e; Matsuda et al., 2009b). To investigate the ionization dynamics of cluster cations, IRPDS-VUV-PI, which is IR predissociation spectroscopy for cluster cations, is carried out by introduction of an IR light pulse after the VUV photoionization process. Under 118 nm (10.5 eV) photon irradiation, the vibrational characteristics of the cluster cations interpreted by theoretical calculations are used to identify the proton-transfer/migration path and process. In addition, the fragmentation mechanisms and thermodynamic properties of these cluster cations can be deciphered in more detail (Matsuda et al., 2006).

Taking acetic acid dimer cations as the example, six stable conformers ($\text{VI}^+ - \text{I}^+$) were found by optimizing at PBE/PBE/6-311 + G(2d,2p) level (Guan et al., 2012b). Matsuda et al. (Ohta et al., 2009) using the IRPDS-VUV-PI technique finds that structures V^+ and IV^+ are the dominant structures for $(\text{CH}_3\text{COOH})_2^+$ irradiated by 10.5 eV photons. Two fragments, the protonated ions $(\text{CH}_3\text{COOH})_{n-1}\text{H}^+$ and the fragment ions $(\text{CH}_3\text{COOH})_{n-1}-\text{COOH}^+$, are considered to be related to the same neutral cluster precursor. Figure 15 displays mass selective IRPD spectra of the $(\text{CH}_3\text{COOH}-\text{COOH})^+$ ions and sequences of the protonated acetic acid clusters $(\text{CH}_3\text{COOH})_n\text{H}^+$ ($n = 1 - 7$) in the C–H and O–H stretch region. Three features in the IR spectra correspond to each other very well for the cations $(\text{CH}_3\text{COOH}-\text{COOH})^+$ and $\text{CH}_3\text{COOH}_2^+$, implying that the ion $(\text{CH}_3\text{COOH}-\text{COOH})^+$ can dissociate to the ion $\text{CH}_3\text{COOH}_2^+$ by losing CO_2 under IR radiation. A dip feature related to the free OH stretch was observed at *ca.* 3,570 cm^{-1} in the IR spectrum of $(\text{CH}_3\text{COOH})_2\text{H}^+$, which suggests a relative stable and closed shell symmetric structure; that is, two acetic acid molecules in the protonated dimer cation $(\text{CH}_3\text{COOH})_2\text{H}^+$ share

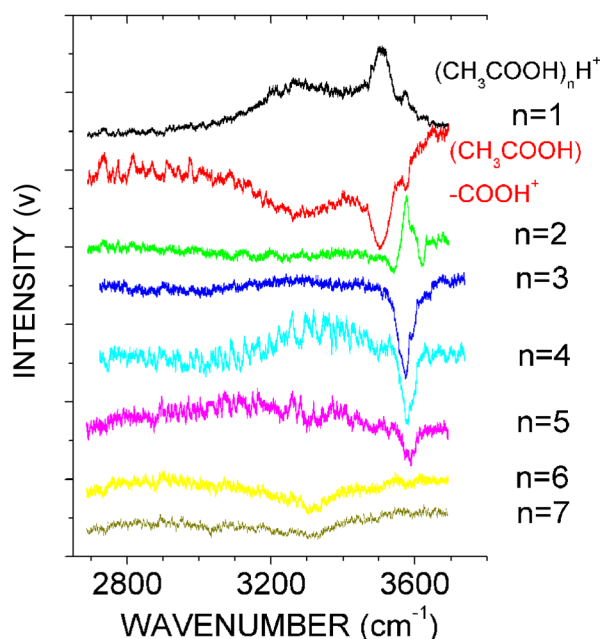


FIGURE 15. Mass selective IRPD spectra of $(\text{CH}_3\text{COOH}-\text{COOH})^+$ ions and sequences of protonated acetic acid clusters $(\text{CH}_3\text{COOH})_n\text{H}^+$ ($n = 1-7$) in the C–H and O–H stretch region.

one proton equally. While the medium size protonated clusters ($n = 3-5$) can be assigned similar structures based on the observation of sharp features around $3,580\text{ cm}^{-1}$ in the IR spectra, these features disappear at $n = 6$, while a weak and broad band is observed at *ca.* $3,320\text{ cm}^{-1}$. The latter indicates closed cyclic or multi-cyclic structures are formed in larger protonated clusters ($n \geq 6$).

Very recently, ionization dynamics and fragmentation mechanisms of acetic acid dimer cations have been accessed by measurement of photoionization onsets and mass spectra of these fragments under a tunable synchrotron VUV radiation (Guan et al., 2012b). By scanning photoionization efficiency (PIE) spectra (see Fig. 16), appearance energies (AEs) of the fragments $(\text{CH}_3\text{COOH})\cdot\text{H}^+$ and $(\text{CH}_3\text{COOH})\text{H}^+(\text{COO})$ were obtained at 10.55 ± 0.05 and 10.34 ± 0.05 eV ionization energy, respectively. Comparing the theoretical calculations with the experimental results, Guan et al. considered that five identified acetic acid dimer cations fragmented through seven competitive paths, as depicted in Figure 17. While four isomers are found to generate the protonated species, only one isomer can dissociate into the C-C bond cleavage product $(\text{CH}_3\text{COOH})\text{H}^+\cdot\text{COO}$. After surmounting the methyl hydrogen transfer barrier at 10.84 ± 0.05 eV, identified in PIE spectra of the fragments $(\text{CH}_3\text{COOH})\cdot\text{H}^+$ and $(\text{CH}_3\text{COOH})\text{H}^+\cdot\text{COO}$, opening of the dissociative channel to produce ions $(\text{CH}_3\text{COOH})^+$ became the most intense fragmentation channel. The opening of this channel

consumed some of precursors of $(\text{CH}_3\text{COOH})\cdot\text{H}^+$ and $(\text{CH}_3\text{COOH})\text{H}^+\cdot\text{COO}$, leading to short flat portions or a slow incline in the PIE spectra. When the photon energy is increased to 12.4 eV, the cations are fragmented and generate new cations $(\text{CH}_3\text{COOH})\cdot\text{CH}_3\text{CO}^+$. Kinetics, thermodynamics, and entropy factors in this work have given a good explanation of these competitive dissociation pathways.

VI. SUMMARY AND OUTLOOK

Vacuum ultraviolet (VUV) radiation provides a convenient soft ionization method for mass spectrometry. This method has been exploited for many detection schemes, which have been employed for vibrational spectroscopic investigations of various molecules, neutral clusters, and cluster cations based on the VUV single photon ionization. These schemes can be helpful to visualize the structure of molecules and their clusters, and elucidate ionization dynamics of molecular clusters. On the other hand, as a new method to detect free radicals, IR-VUV photoionization spectroscopy also has the unique advantage of mass selectivity.

The molecules and clusters discussed in this review are specifically selected to have ionization energy (IP) around 10.5 eV (i.e., single photo energy of 118 nm) because this photon energy is most easily generated and at the highest current intensity. For further and general applications of the present

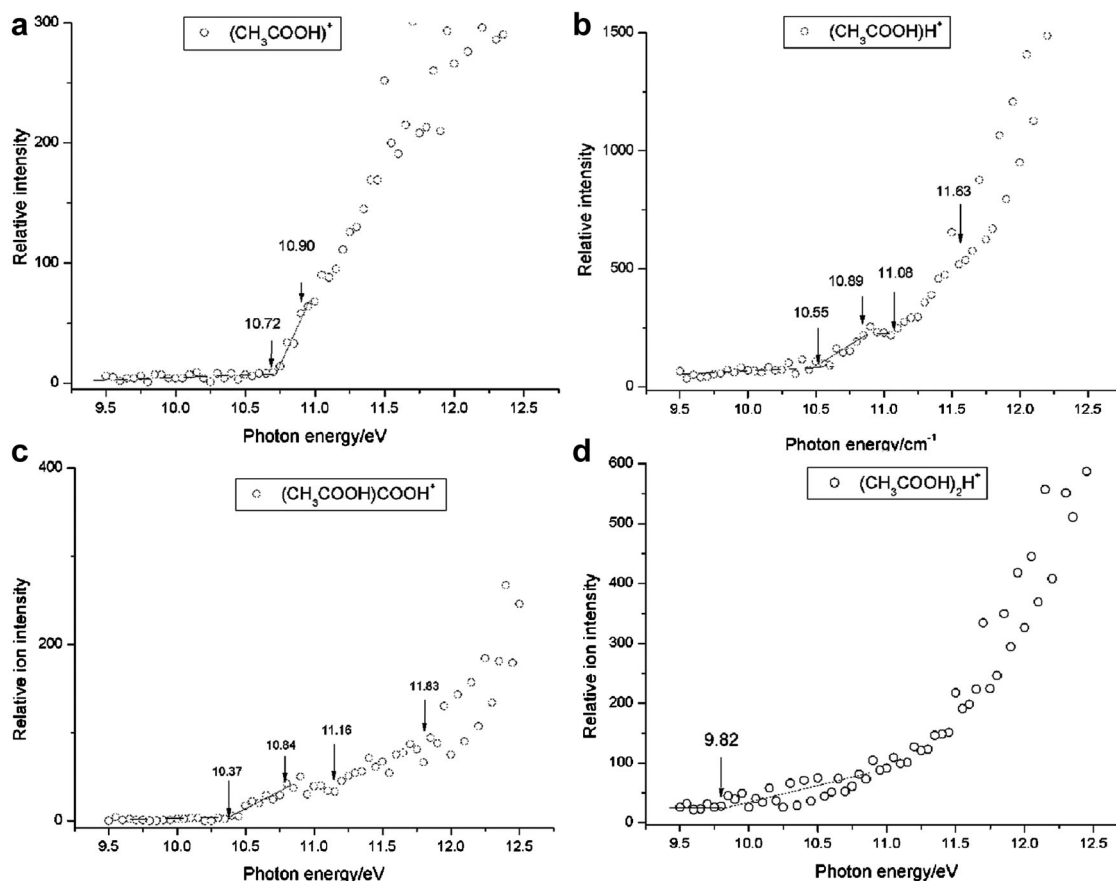


FIGURE 16. PIE spectra of (a) the acetic acid cation $(\text{CH}_3\text{COOH})^+$, (b)-(c) protonated acetic acid clusters $(\text{CH}_3\text{COOH})_n\text{H}^+$ ($n = 1, 2$) and (d) fragment $(\text{CH}_3\text{COOH-COOH})^+$ ions.

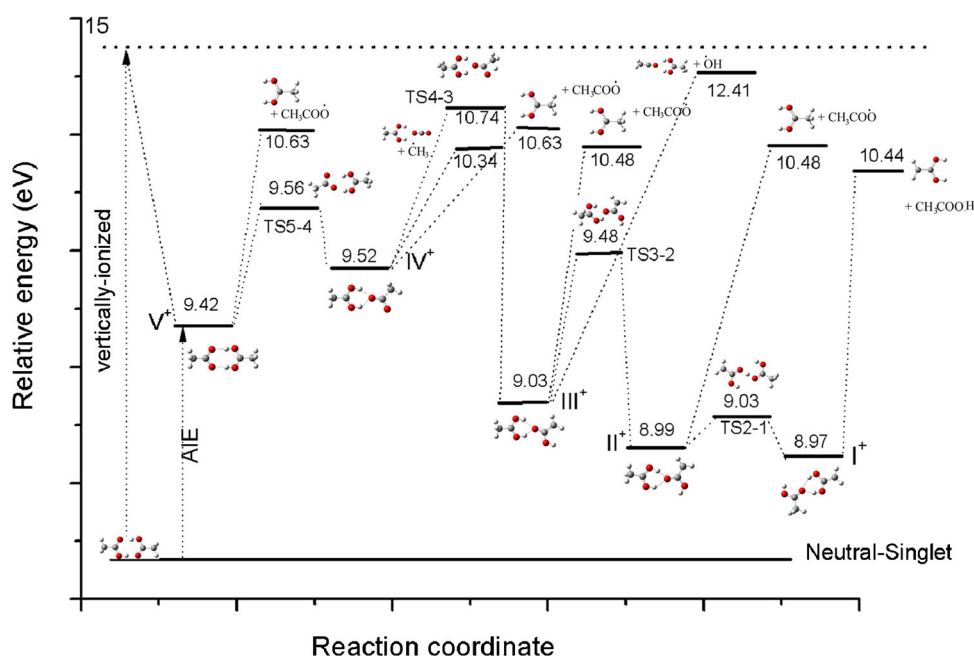


FIGURE 17. Seven competitive fragmentation channels for the acetic acid dimer cation under VUV radiation.

spectroscopic schemes, tunable VUV light for soft ionization of all molecules and selective ionization for all isomers are necessary. Furthermore, high resolution and a wide range IR radiation source (e.g., free electron laser (FEL)) (Oomens, Steill, & Redlich, 2009; Ullrich, Rudenko, & Moshhammer, 2012) would be highly useful to employ for resolving vibration, rovibration, and electronic transitions. With the improved detection sensitivity and the tunable VUV and IR radiation range, IR plus VUV spectroscopy would have a broad application for spectroscopic characterization of molecular interactions, cluster structure, and unstable species. Spectroscopic tracking of structural evolution of molecules under isolated circumstances is possible, as well, with advanced ultrafast vibrational spectroscopy. With the aid of theoretical calculations, these experimental techniques can also be used to explore the fragmentation kinetics of clusters under VUV photoionization and dissociation, and to understand their ionization dynamics and competitive fragmentation mechanisms in high energy collisional activation experiments.

ACKNOWLEDGMENTS

This work has been supported by National Natural Science Foundation of China (no. 20973067, 11079020, 21273083) and the scientific research foundation for the returned overseas Chinese scholars, State Education Ministry. The experimental work for most of these studies was initiated at Colorado State University under the support of the U.S. Army Research Office and the National Science Foundation.

REFERENCES

Abo-Riziq A, Crews BO, Callahan MP, Grace L, de Vries MS. 2006. Gas phase spectroscopy of the penta-peptide FDASV. *Chem Phys Lett* 431:227–230.

Ashfold MNR, Clement SG, Howe JD, Western CM. 1993. Multiphoton ionisation spectroscopy of free radical species. *J Chem Soc Faraday Trans* 89:1153–1172.

Bahng MK, Xing X, Baek SJ, Qian X, Ng CY. 2006. A combined VUV synchrotron pulsed field ionization-photoelectron and IR-VUV laser photoion depletion study of ammonia. *J Phys Chem A* 110:8488–8496.

Belau L, Wilson KR, Leone SR, Ahmed M. 2007. Vacuum ultraviolet (VUV) photoionization of small water clusters. *J Phys Chem A* 111:10075–10083.

Bhattacharya A, Shin JW, Clawson KJ, Bernstein ER. 2010. Conformation specific and charge directed reactivity of radical cation intermediates of alpha-substituted (amino, hydroxy, and keto) bioactive carboxylic acids. *Phys Chem Chem Phys* 12:9700–9712.

Bieske EJ, Dopfer O. 2000. High-resolution spectroscopy of cluster ions. *Chem Rev* 100:3963–3998.

Bjorklund GC. 1975. Effects of focusing on third-order nonlinear processes in isotropic media. *IEEE J Quantum Electron* QE 11:287–296.

Brodbeck JS, Wilson JJ. 2009. Infrared multiphoton dissociation in quadrupole ion traps. *Mass Spectrom Rev* 28(3):309–424.

Brutschy B. 2000a. The structure of microsolvated benzene derivatives and the role of aromatic substituents. *Chem Rev* 100:3891–3920.

Brutschy B. 2000b. Van der Waals molecules III: Introduction. *Chem Rev* 100:3861–3862.

Buck U, Huysken F. 2000. Infrared spectroscopy of size-selected water and methanol clusters. *Chem Rev* 100:3863–3890.

Buzza SA, Snyder EM, Castleman AW. 1996. Further direct evidence for stepwise dissociation of acetone and acetone clusters. *J Chem Phys* 104:5040–5048.

Calvert JG, Lazrus A, Kok GL, Heikes BG, Walega JG, Lind J, Cantrell CA. 1985. Chemical mechanisms of acid generation in the troposphere. *Nature* 317:27–35.

Cao XL, Fischer G. 2000. Infrared spectra of monomeric L-alanine and L-alanine-N-d(3) zwitterions isolated in a KBr matrix. *Chem Phys* 255:195–204.

Chervenkov S, Wang PQ, Braun JE, Neusser HJ. 2004. Fragmentation and conformation study of ephedrine by low- and high-resolution mass selective UV spectroscopy. *J Chem Phys* 121:7169–7175.

- Chin W, Piuze F, Dognon JP, Dimicoli I, Tardivel B, Mons M. 2005. Gas phase formation of a 3_{10} -helix in a three-residue peptide chain: Role of side chain-backbone interactions as evidenced by IR-UV double resonance experiments. *J Am Chem Soc* 127:11900–11901.
- Chin W, Piuze F, Dimicoli I, Mons M. 2006. Probing the competition between secondary structures and local preferences in gas phase isolated peptide backbones. *Phys Chem Chem Phys* 8:1033–1048.
- Claeys M, Graham B, Vas G, Wang W, Vermeylen R, Pashynska V, Cafmeyer J, Guyon P, Andreae MO, Artaxo P, Maenhaut W. 2004. Formation of secondary organic aerosols through photooxidation of isoprene. *Science* 303:1173–1176.
- Dessent CEH, Müller-Dethlefs K. 2000. Hydrogen-bonding and van der Waals complexes studied by ZEKE and REMPI spectroscopy. *Chem Rev* 100:3999–4022.
- Diken EG, Headrick JM, Roscioli JR, Bopp JC, Johnson MA, McCoy AB. 2005. Fundamental excitations of the shared proton in the H_3O^+ and $H_5O_2^+$ complexes. *J Phys Chem A* 109:1487–1490.
- Dong F, Heinbuch S, Rocca JJ, Bernstein ER. 2006. Dynamics and fragmentation of van der Waals clusters: $(H_2O)_n$, $(CH_3OH)_n$, and $(NH_3)_n$ upon ionization by a 26.5 eV soft x-ray laser. *J Chem Phys* 124:224319–224336.
- Duncan MA. 2003. Infrared spectroscopy to probe structure and dynamics in metal ion-molecule complexes. *Int Rev Phys Chem* 22:407–435.
- Ebata T, Fujii A, Mikami N. 1998. Vibrational spectroscopy of small-size hydrogen-bonded clusters and their ions. *Int Rev Phys Chem* 17:331–361.
- Fu HB, Hu YJ, Bernstein ER. 2005. IR/UV double resonant spectroscopy of the methyl radical: Determination of ν_3 in the $3p_z$ Rydberg state. *J Chem Phys* 123:234307–234312.
- Fu HB, Hu YJ, Bernstein ER. 2006a. IR + vacuum ultraviolet (118 nm) nonresonant ionization spectroscopy of methanol monomers and clusters: Neutral cluster distribution and size-specific detection of the OH stretch vibrations. *J Chem Phys* 124:024302–024309.
- Fu HB, Hu YJ, Bernstein ER. 2006b. Generation and detection of alkyl peroxy radicals in a supersonic jet expansion. *J Chem Phys* 125:014310–014317.
- Gerhards M. 2004. High energy and narrow bandwidth mid IR nanosecond laser system. *Opt Commun* 241:493–497.
- Gerhards M, Unterberg C, Gerlach A. 2002. Structure of a β -sheet model system in the gas phase: Analysis of the CO stretching vibrations. *Phys Chem Chem Phys* 4:5563–5565.
- Grotheer HH, Nomayo M, Pokorny H, Thanner R, Gullett BK. 2001. Wavelength-resolved REMPI mass spectrometry for the monitoring of toxic incineration trace gases. *Trends Appl Spectrosc* 3:181–206.
- Guan JW, Hu YJ, Xie M, Bernstein ER. 2012a. Weak carbonyl-methyl intermolecular interactions in acetone clusters explored by IR plus VUV spectroscopy. *Chem Phys* 405:117–123.
- Guan JW, Hu YJ, Zou H, Cao L, Liu FY, Shan XB, Sheng LS. 2012b. Competitive fragmentation pathways of acetic acid dimer explored by synchrotron VUV photoionization mass spectrometry and electronic structure calculations. *J Chem Phys* 137:124308–124317.
- Guo YQ, Bhattacharya A, Bernstein ER. 2009. Photodissociation dynamics of nitromethane at 226 and 271 nm at both nanosecond and femtosecond time scales. *J Phys Chem A* 113:85–96.
- Haber T, Seefeld K, Kleinermanns K. 2007. Mid- and near-infrared spectra of conformers of H-Pro-Trp-OH. *J Phys Chem A* 111:3038–3046.
- Hagemeister FC, Gruenloh CJ, Zwier TS. 1998. Density functional theory calculations of the structures, binding energies, and infrared spectra of methanol clusters. *J Phys Chem A* 102:82–94.
- Han HL, Camacho C, Witek HA, Lee YP. 2011a. Infrared absorption of methanol clusters $(CH_3OH)_n$ with $n = 2$ –6 recorded with a time-of-flight mass spectrometer using infrared depletion and vacuum-ultraviolet ionization. *J Chem Phys* 134:144309–144320.
- Han HL, Fu L, Lee YP. 2011b. Infrared spectrum of mass-selected CH_3S radicals investigated with infrared + vacuum ultraviolet photoionization. *Chem Phys Lett* 515:1–6.
- Hanley L, Zimmermann R. 2009. Light and molecular ions: The emergence of vacuum UV single-photon ionization in MS. *Anal Chem* 81:4174–4182.
- Hart DJ, Bourne OL, Rayner DM. 1989. Narrow bandwidth coherent VUV spectroscopy of the Kr 123.58 nm line. *Opt Commun* 73:213–216.
- Headrick JM, Bopp JC, Johnson MA. 2004. Predissociation spectroscopy of sequence information in collision-induced dissociation of peptides. *J Am Chem Soc* 128:10364–10365.
- Heinbuch S, Dong F, Rocca JJ, Bernstein ER. 2007. Single photon ionization of hydrogen bonded clusters with a soft x-ray laser: $(HCOOH)_x$ and $(HCOOH)_y(H_2O)_z$. *J Chem Phys* 126:244301–244312.
- Hepburn JW. 1994. ??? In: Meyers A, Rizzo TR, editors. *Laser techniques in chemistry*. New York: Wiley. pp 149–183.
- Hilbig R, Wallenstein R. 1983. Tunable XUV radiation generated by nonresonant frequency tripling in argon. *Opt Commun* 44:283–288.
- Hu YJ, Bernstein ER. 2008. Vibrational and photoionization spectroscopy of biomolecules: Aliphatic amino acid structures. *J Chem Phys* 128:164311–164321.
- Hu YJ, Bernstein ER. 2009a. Vibrational and photoionization spectroscopy of neutral valine clusters. *J Phys Chem A* 113:8454–8461.
- Hu YJ, Bernstein ER. 2009b. Photoionization and vibrational spectroscopy of aniline-methanol clusters. *J Phys Chem A* 113:639–643.
- Hu YJ, Fu HB, Bernstein ER. 2006a. IR plus VUV spectroscopy of neutral and ionic ethanol monomers and small clusters. *J Chem Phys* 125:154305–154311.
- Hu YJ, Fu HB, Bernstein ER. 2006b. IR plus VUV spectroscopy of neutral and ionic methanol monomers and clusters: New experimental results. *J Chem Phys* 125:154306–154311.
- Hu YJ, Fu HB, Bernstein ER. 2006c. IR plus VUV spectroscopy of neutral and ionic organic acid molecules and clusters: Propanoic acid. *J Chem Phys* 125:184309–184316.
- Hu YJ, Fu HB, Bernstein ER. 2006d. Vibronic spectroscopy of the peroxyacetyl radical in the near IR. *J Chem Phys* 124:114305–114311.
- Hu YJ, Fu HB, Bernstein ER. 2006e. IR plus VUV spectroscopy of neutral and ionic organic acid molecules and clusters: Acetic acid. *J Chem Phys* 125:184308–184315.
- Hu YJ, Fu HB, Bernstein ER. 2006f. Generation and detection of the peroxyacetyl radical in the pyrolysis of peroxyacetyl nitrate in the supersonic expansion. *J Phys Chem A* 110:2629–2633.
- Hunig I, Kleinermanns K. 2004. Conformers of the peptides glycine-tryptophan, tryptophan-glycine and tryptophan-glycine-glycine as revealed by double resonance laser spectroscopy. *Phys Chem Chem Phys* 6:2650–2658.
- Hunt RH, Shelton WN, Flaherty FA, Cook WB. 1998. Torsion-rotation energy levels and the hindering potential barrier for the excited vibrational state of the OH-stretch fundamental band ν_1 of methanol. *J Mol Spectrosc* 192:277–293.
- Ishiyuchi S, Shitomi H, Takazawa K, Fujii M. 1998. Nonresonant ionization detected IR spectrum of jet-cooled phenol-ionization mechanism and its application to overtone spectroscopy. *Chem Phys Lett* 283:243–250.
- Jiang S, Levy DH. 2002. Supersonic jet studies on the photophysics of substituted benzenes and naphthalene. *J Phys Chem A* 106:8590–8598.
- Jin Z, Daiya S, Kenttämäa HI. 2011. Characterization of nonpolar lipids and selected steroids by using laser-induced acoustic desorption/chemical ionization, atmospheric pressure chemical ionization, and electrospray ionization mass spectrometry. *Int J Mass Spectrom* 301:234–239.
- Jockusch RA, Kroemer RT, Talbot FO, Snoek LC, Carcabal PJ, Simons P, Havenith M, Bakker JM, Compagnon I, Meijer G, von Helden G. 2004. Probing the glycosidic linkage: UV and IR ion-dip spectroscopy of a lactoside. *J Am Chem Soc* 126:5709–5714.
- Kaczor A, Reva ID, Proniewicz LM, Fausto R. 2006. Importance of entropy in the conformational equilibrium of phenylalanine: A matrix-isolation infrared spectroscopy and density functional theory study. *J Phys Chem A* 110:2360–2370.

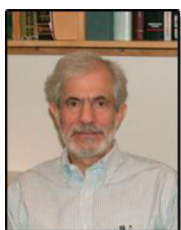
- Kohn DW, Clauberg H, Chen P. 1992. Flash pyrolysis nozzle for generation of radicals in a supersonic jet expansion. *Rev Sci Instrum* 63:4003–4006.
- Kung AH. 1983. Third-harmonic generation in a pulsed supersonic jet of xenon. *Opt Lett* 8:24–26.
- Kung AH, Lee YT. 1991. Spectroscopy and reaction dynamics using ultrahigh resolution VUV lasers. Ng CY, editor. In *vacuum ultraviolet photoionization and photodissociation of molecules and clusters*. Singapore: World Scientific. pp 487–502.
- Lee YT, McDonald JD, LeBreton PR, Herschbach DR. 1969. Molecular beam reactive scattering apparatus with electron bombardment detector. *Rev Sci Instrum* 40:1402–1408.
- Lee SY, Shin DN, Cho SG, Jung KH, Woo JK. 1995. Proton-transfer reactions within ionized methanol clusters: Mass spectrometric and molecular orbital studies. *J Mass Spectrom* 30:969–976.
- Lee KT, Sung JL, Lee KJ, Park YD, Kim SK. 2002. Conformation-dependent ionization energies of L-phenylalanine. *Angew Chem Int Ed* 41:4114–4117.
- Lipson RH, Dimov SS, Wang P, Shi YJ, Mao DM, Hu XK, Vanstone J. 2000. Vacuum ultraviolet and extreme ultraviolet lasers: Principles instrumentation and applications. *Instrum Sci Technol* 28:85–118.
- Lisy JM. 2006. Infrared studies of ionic clusters: The influence of Yuan T. Lee. *J Chem Phys* 125:132302–132321.
- MacAleese L, Maitre P. 2007. Infrared spectroscopy of organometallic ions in the gas phase: From model to real world complexes. *Mass Spectrom Rev* 26:583–605.
- Matsuda Y, Mori M, Hachiya M, Fujii A, Mikami N. 2006. Infrared spectroscopy of size-selected neutral clusters combined with vacuum-ultraviolet-photoionization mass spectrometry. *Chem Phys Lett* 422:378–381.
- Matsuda Y, Hachiya M, Fujii A, Mikami N. 2007. Stimulated Raman spectroscopy combined with vacuum ultraviolet photoionization: Application to jet-cooled methanol clusters as a new vibrational spectroscopic method for size-selected species in the gas phase. *Chem Phys Lett* 442:217–219.
- Matsuda Y, Ohta K, Mikami N, Fujii A. 2009a. Infrared spectroscopy for acetone and its dimer based on photoionization detection with tunable coherent vacuum-ultraviolet light. *Chem Phys Lett* 471:50–53.
- Matsuda Y, Mikami N, Fujii A. 2009b. Vibrational spectroscopy of size-selected neutral and cationic clusters combined with vacuum-ultraviolet one-photon ionization detection. *Phys Chem Chem Phys* 11:1279–1290.
- Matsuda Y, Yamada A, Hanaue K, Mikami N, Fujii A. 2010. Catalytic action of a single water molecule in a proton-migration reaction. *Angew Chem Int Ed* 49:4898–4901.
- Moxim WJ, Levy H, Kasibhatla PS. 1996. Simulated global tropospheric PAN: Its transport and impact on NOx. *J Geophys Res* 101:12621–12638.
- Myers LE, Eckhardt RC, Fejer MM, Beyer RL, Bosenberg WR, Pierce JW. 1995. Quasi-phase-matched optical parametric oscillators in bulk periodically poled LiNbO3. *J Opt Soc Am B* 12:1202–2116.
- Ng CY. 2000. Molecular beam photoionization studies of molecules and applications. *Int J Mass Spectr* 200:357–386.
- Ng CY. 2002. Vacuum ultraviolet spectroscopy and chemistry using photoionization and photoelectron methods. *Annu Rev Phys Chem* 53:101–140.
- Ng CY. 2009. Spectroscopy and dynamics of neutrals and ions by high-resolution infrared-vacuum ultraviolet photoionization and photoelectron methods. Laane J, editor. *Frontiers of molecular spectroscopy*. Amsterdam: Elsevier Science and Technology. pp 659–691.
- Ohta K, Matsuda Y, Mikami N, Fujii A. 2009. Intermolecular proton-transfer in acetic acid clusters induced by vacuum-ultraviolet photoionization. *J Chem Phys* 131:184304–184315.
- Oomens J, Steill JD, Redlich B. 2009. Gas-phase IR spectroscopy of deprotonated amino acids. *J Am Chem Soc* 131:4310–4319.
- Polfer NC, Oomens J. 2009. Vibrational spectroscopy of bare and solvated ionic complexes of biological relevance. *Mass Spectrom Rev* 28:468–494.
- Rettner CT, Marinero EE, Zare RN, Kung AH. 1984. Pulsed Free Jets: Novel nonlinear media for generation of vacuum ultraviolet and extreme ultraviolet radiation. *J Phys Chem* 88:4459–4465.
- Rueda D, Boyarkin OV, Rizzo TR, Chirokolava A, Perry DS. 2005. Vibrational overtone spectroscopy of jet-cooled methanol from 5000 to 14 000 cm⁻¹. *J Chem Phys* 122:044314–044322.
- Ryan WL, Levy DH. 2001. Electronic spectroscopy and photoisomerization of trans-urocanic acid in a supersonic jet. *J Am Chem Soc* 123:961–966.
- Ryan WL, Gordon DJ, Levy DH. 2002. Gas-phase photochemistry of the photoactive yellow protein chromophore trans-p-coumaric acid. *J Am Chem Soc* 124:6194–6201.
- Shang QY, Moreno PQ, Bernstein ER. 1994. Synthesis and reactivity of a stable hydrido bis(dihydrogen) derivative in a nitrogen donor environment LRuH(H₂)₂ (L = HB(3,5-Me₂-pz), HB(3-iPr,4-Br-pz)). *J Am Chem Soc* 116:2635–2636.
- Shi YJ, Hu XK, Mao DM, Dimov SS, Lipson RH. 1998. Analysis of xanthate derivatives by vacuum ultraviolet laser-time-of-flight mass spectrometry. *Anal Chem* 70:4534–4539.
- Shi YJ, Consta S, Das AK, Mallik B, Lacey D, Lipson RH. 2002. A 118 nm vacuum ultraviolet laser/time-of-flight mass spectroscopic study of methanol and ethanol clusters in the vapor phase. *J Chem Phys* 116:6990–7000.
- Softley TP, Ernst WE, Tashiro LM, Zare RN. 1987. A general-purpose xuv laser spectrometer-some applications to N₂, O₂ and CO₂. *Chem Phys* 116:299–309.
- Stepanian SG, Reva ID, Radchenko ED, Adamowicz L. 2001. Conformers of nonionized praline: Matrix-isolation infrared and post-Hartree-Fock ab initio study. *J Phys Chem A* 105:10664–10672.
- Svec HJ, Clyde DD. 1965. Vapour pressures of some α-amino acids. *J Chem Eng Data* 10:151–152.
- Takayama M. 1996. Gas-phase fast-atom bombardment mass spectrometry. *Int J Mass Spectrom Ion Processes* 152:1–20.
- Tsai ST, Jiang JC, Lin MF, Lee YT, Ni CK. 1999. Photoionization of methanol dimer using a tunable vacuum ultraviolet laser. *J Chem Phys* 111:3434–3440.
- Ullrich J, Rudenko A, Moshhammer R. 2012. Free-electron lasers: New avenues in molecular physics and photochemistry. *Annu Rev Phys Chem* 63:635–660.
- Woo HK, Wang P, Lau KC, Xing X, Chang C, Ng CY. 2003. State-selected and state-to-state photoionization study of trichloroethene using the two-color infrared-vacuum ultraviolet scheme. *J Chem Phys* 119:9333–9337.
- Woodward JR, Watanabe H, Ishiuchi S, Fujii M. 2012. A two-color tunable infrared/vacuum ultraviolet spectrometer for high-resolution spectroscopy of molecules in molecular beams. *Rev Sci Instrum* 83:014102–014111.
- Yamada Y, Okano J, Mikami N, Ebata T. 2005. Picosecond IR-UV pump-probe spectroscopic study on the intramolecular vibrational energy redistribution of NH₂ and CH stretching vibrations of jet-cooled aniline. *J Chem Phys* 123:124316–124325.
- Yamanouchi K, Tsuchiya S. 1995. Tunable vacuum ultraviolet laser spectroscopy: Excited state dynamics of jet-cooled molecules and van der Waals complexes. *J Phys B At Mol Opt Phys* 28:133–165.
- Zwier TS. 1996. The spectroscopy of solvation in hydrogen-bonded aromatic clusters. *Annu Rev Phys Chem* 47:205–241.



Yong-Jun Hu graduated in the Department of Environmental Science of Nankai University in 1994, and received a doctorate degree of science from Chinese Academy of Science in 2000. He was a postdoctoral researcher in Hebrew University of Jerusalem from 2000 to 2003 and in Colorado State University from 2003 to 2006. He is now a professor in MOE Key Laboratory of Laser Life Science, South China Normal University in Guangzhou. His research interests are laser spectroscopy studies of molecular geometric and electronic structure, intermolecular interactions, and photoionization dynamics of molecules and clusters in the gas phase.



Ji-Wen Guan received his B.S. in 2010 from College of Physical Science and Technology, Yangtze University in Hubei province, China. He is finishing his M.S. thesis in the MOE Key Laboratory of Laser Life Science, South China Normal University in Guangzhou under the guidance of Prof. Yong-Jun Hu. His research interest is mass-selective IR spectroscopy of molecules and clusters using IR-VUV photoionization techniques, as well as VUV photoionization and dissociation of jet-cooled species.



Elliot R. Bernstein graduated from Princeton University and has a Ph.D. from California Institute of Technology. He conducted postdoctoral research at Enrico Fermi Institute, University of Chicago and became an assistant professor in Department of Chemistry, Princeton University in 1969. He is now a professor in the Department of Chemistry, Colorado State University. His research concerns intermolecular interactions and their manifestations through optical spectroscopy of gas phase molecular and covalent clusters. The particular systems of interest have been organic solute/solvent clusters, solvated organic radicals, and metal and metal compound clusters. Both energy levels and dynamics of these clusters are investigated experimentally and theoretically. Chemical reactions, reaction dynamics, and catalysis are also studied for radical, inorganic, and solute/solvent clusters.